CHEMISTRY
A EUROPEAN JOURNAL

DOI: 10.1002/chem.201002635

Selectivity among Two Lectins: Probing the Effect of Topology, Multivalency and Flexibility of "Clicked" Multivalent Glycoclusters

Samy Cecioni,[a, b] Sophie Faure,[c] Ulrich Darbost,[d] Isabelle Bonnamour,[d] Hélène Parrot-Lopez,[d] Olivier Roy,[c] Claude Taillefumier,[c] Michaela Wimmerová,[e] Jean-Pierre Praly,[a] Anne Imberty,[b] and Sébastien Vidal*[a]

Abstract: The design of multivalent glycoconjugates has been developed over the past decades to obtain high-affinity ligands for lectin receptors. While multivalency frequently increases the affinity of a ligand for its lectin through the so-called "glycoside cluster effect", the binding profiles towards different lectins have been much less investigated. We have designed a series of multivalent galactosylated glycoconjugates and studied their binding properties towards two lectins, from plant and bacterial origins, to determine their potential selectivity. The synthesis was achieved through copper(I)-catalysed azide–alkyne cycloaddition (CuAAC) under microwave activation between propargylated multivalent scaffolds and an azido-functionalised carbohydrate derivative. The interactions of two galactose-binding lectins from *Pseudomonas aeruginosa* (PA-IL) and *Erythrina cristagalli* (ECA) with the synthesized glycoclusters were studied by hemagglutination inhibition assays (HIA), surface plasmon resonance (SPR) and isothermal titration microcalorimetry (ITC). The results obtained illustrate the influence of the scaffold's geometry on the affinity towards the lectin and also on the relative potency in comparison with a monovalent galactoside reference probe.

Keywords: calixarenes · carbohydrates · glycoclusters · lectins · multivalency

Introduction

The interactions between lectins and carbohydrates play a central role in a large number of biological processes, such as cell–cell communication, cell adhesion, cell recognition, cell differentiation, host–pathogen interactions, signal transduction, intracellular trafficking of proteins, inflammation, metastasis and development of the neuronal network. The affinity of lectins for their substrate is usually relatively weak with typical dissociation constants in the millimolar range.[1] The clustering of receptors at the surface of the cell and/or the multivalent display of carbohydrate epitopes am-

[a] S. Cecioni, Dr. J.-P. Praly, Dr. S. Vidal
Institut de Chimie et Biochimie Moléculaires et Supramoléculaires, Laboratoire de Chimie Organique 2 - Glycochimie, UMR5246
Université Claude Bernard Lyon 1 and CNRS
43 Boulevard du 11 Novembre 1918
69622, Villeurbanne (France)
Fax: (+33) 472-431-184
E-mail: sebastien.vidal@univ-lyon1.fr

[b] S. Cecioni, Dr. A. Imberty
CERMAV - CNRS, affiliated with Université Joseph Fourier and ICMG, BP 53, 38041
Grenoble Cedex 9 (France)

[c] Dr. S. Faure, Dr. O. Roy, Dr. C. Taillefumier
Clermont Université, Université Blaise Pascal
Laboratoire SEESIB, BP 10448, F-63000 Clermont-Ferrand and CNRS, UMR 6504, Laboratoire SEESIB
63177 Aubière cedex (France)

[d] Dr. U. Darbost, Dr. I. Bonnamour, Dr. H. Parrot-Lopez
Institut de Chimie et Biochimie Moléculaires et Supramoléculaires, Chimie Supramoléculaire Appliquée (CSAp), UMR 5246
Université Claude Bernard Lyon 1 and CNRS
43 Boulevard du 11 Novembre 1918
69622, Villeurbanne (France)

[e] Dr. M. Wimmerová
National Centre for Biomolecular Research and Department of Biochemistry, Faculty of Science
Masaryk University, Kotlářská 2
611 37 Brno (Czech Republic)

Supporting information for this article is available on the WWW under http://dx.doi.org/10.1002/chem.201002635.

WILEY ONLINE LIBRARY

© 2011 Wiley-VCH Verlag GmbH & Co. KGaA, Weinheim

plifies drastically the strength of the interaction between the partners to reach very selective and stable interactions through the so-called "glycoside cluster effect".[2–4]

The design of multivalent glycoconjugates,[5] such as glycoclusters,[6–11] glycodendrimers,[12–14] glycopolymers,[15–17] and glyconanoparticles[18–22] has brought a large set of data on the binding properties of each class of conjugates with lectins. While the positive influence of multivalency on the affinity to lectins has been clearly demonstrated, the influence of the glycoconjugates' topology on the affinity has been scarcely investigated. Two recent reports demonstrated that calix[4]arene-based glycoconjugates bind differently to a galactose-binding lectin based on their topological patterns.[23,24]

Another approach would be to compare the binding properties of a series of multivalent glycoconjugates to several lectins with different architectures and binding-site topologies.[25–27] Two galactose-binding lectins, from bacteria and plant origin, have been selected for such a comparison. PA-IL is a soluble lectin from *Pseudomonas aeruginosa* that binds to galactose and α-galactose-containing oligosaccharides with medium-range affinity (K_d ~50 μM).[28,29] The crystal structure reveals a tetrameric arrangement with a general rectangular shape.[30] Agglutinin from *Erythrina cristagalli* (ECA) displays weaker affinity for galactose (K_d = 1.25 mM) and lactose (K_d = 300 μM) and assembles in the canonical legume–lectin dimer presenting binding sites at its extremities.[31] Comparison of the lectin architectures and distances between binding sites is displayed in Figure 1.

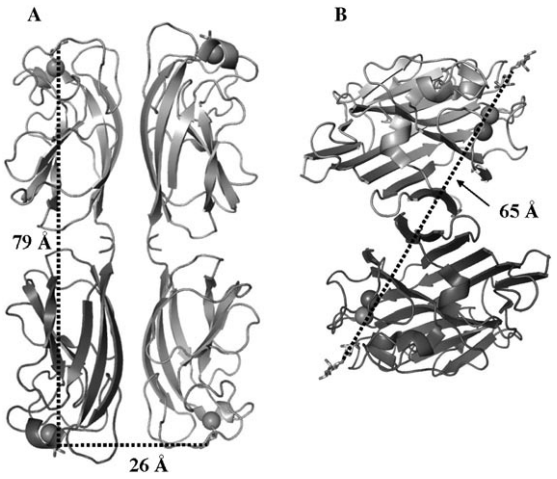

Figure 1. Structures of A) PA-IL in complex with galactose (PDB code 1OKO) and B) ECA in complex with lactose (PDB code 1GZC). The peptide chain is represented as ribbons, metal ions as spheres and carbohydrate ligands as sticks. The distances have been measured from the glycosidic oxygen of bound galactose.

We present here the synthesis of a series of multivalent glycoclusters and their binding properties with lectins presenting different quaternary structures as determined by hemagglutination inhibition assay (HIA), surface plasmon resonance (SPR) and isothermal titration microcalorimetry (ITC).

Results and Discussion

Synthesis of multivalent glycoclusters: The assembly of the multivalent glycoconjugates was performed by using a convergent approach. The copper(I)-catalysed azide–alkyne cycloaddition (CuAAC; "click" chemistry) between propargylated scaffolds and an azido-functionalised carbohydrate probe afforded the corresponding triazolyl cycloadducts.[32–42] The use of microwave irradiation accelerated the 1,3-dipolar cycloaddition process. This methodology is probably among the most efficient in terms of yields, reaction time and chemoselectivity.

β-Peptoids are surrogates of β-peptides in which the side chains are moved from the backbone carbon atoms to the amide nitrogen atoms.[43] We have recently developed a method for the preparation of β-peptoids functionalised with propargyl residues.[44] The efficient solution-phase methodology allowed for the rapid gram-scale synthesis of linear oligomers of valencies up to six. The corresponding cyclic β-peptoids were also synthesized with appended propargyl groups and their functionalisation with azido-derivatised molecules was investigated. We focused here on the synthesis of the tetravalent linear and cyclic oligomers and their conjugation to a carbohydrate probe through "click" chemistry.[45–47] The secondary amine of the linear tetrapropargylated β-peptoid **1**[44] was acetylated and the corresponding acetamide **2** was then conjugated to 1-azido-3,6-dioxaoct-8-yl-2,3,4,6-tetra-*O*-acetyl-β-D-galactopyranoside **A**[40,48] through CuAAC under microwave irradiation to afford the peracetylated glycoconjugate **3** (Scheme 1). Saponification of both the *tert*-butyl ester and acetates afforded the hydroxylated glycocluster **4**. In a similar fashion, the cyclic tetravalent β-peptoid **5** was subjected to our standard "click" chemistry conditions to afford the corresponding glycoconjugate **6** and subsequent solvolysis of the ester groups provided the cyclic glycocluster **7**.

Calix[*n*]arenes are typical scaffolds used for the design of glycoconjugates[23,40,49–55] with, in particular, recent examples of construction of such glycoconjugates through CuAAC.[47] Calix[6]arenes provide interesting scaffolds in which the carbohydrate epitopes will be condensed in a narrow space (although the conformational rigidity of calix[6]arenes is much weaker than for calix[4]arenes) and will create a high-density volume of ligands available for binding to a lectin. To exploit the particularly dense functionalisation of these scaffolds, we have prepared two calix[6]arenes with either three of six propargyl residues and their subsequent condensation with the azido-functionalised carbohydrate probe was achieved by "click" chemistry.

The regioselective trimethylation of calix[6]arene **8**[56]provided **9**[57] and the propargylation of the remaining phenolic positions was achieved with propargyl bromide and sodium hydride in refluxing THF to afford the tripropargy-

 © 2011 Wiley-VCH Verlag GmbH & Co. KGaA, Weinheim

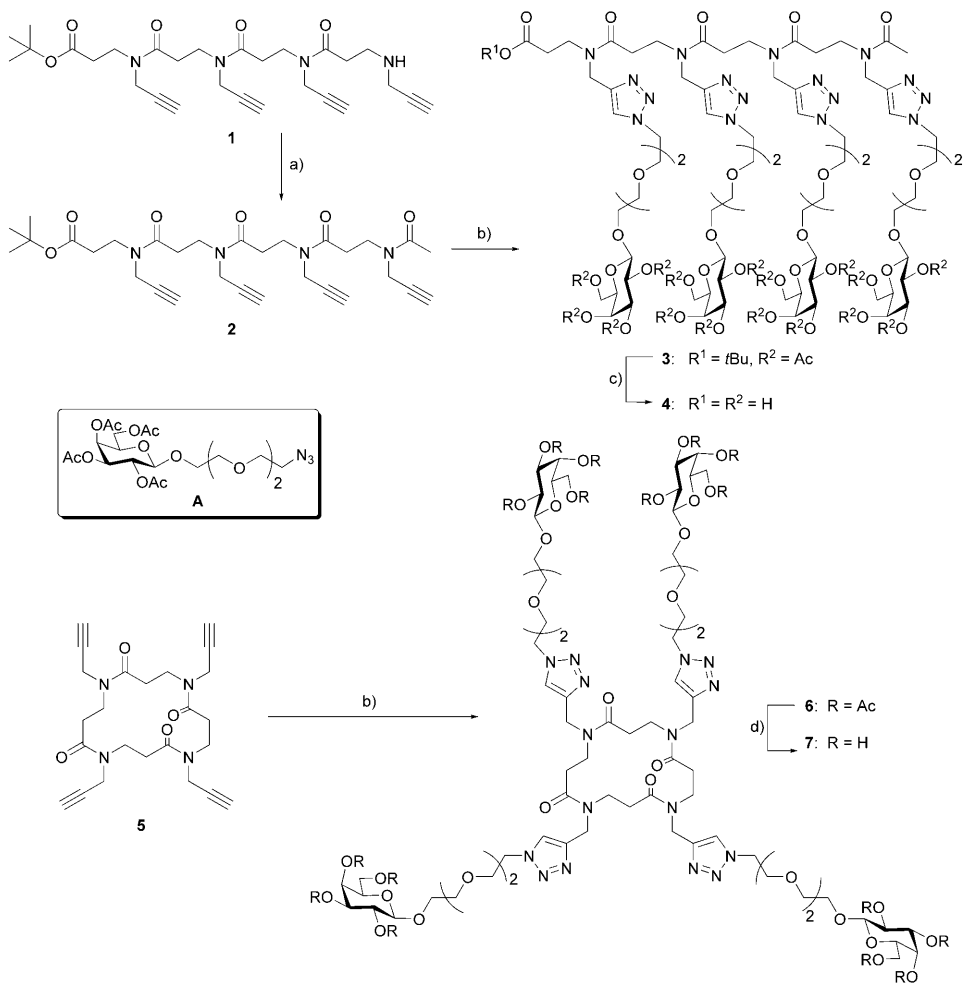

Scheme 1. a) Ac_2O, CH_2Cl_2, RT, 5 h, 97%; b) **A**, CuI, iPr_2NEt, DMF, μW, 110°C, 15 min, 86% for **3**, 77% for **6**; c) NaOH, THF, H_2O, RT, 16 h, 77%; d) $MeOH/Et_3N/H_2O$ (4:1:1), RT, 4 days, 87%.

lated scaffold **10**[58] (Scheme 2). The acetylated glycoconjugate **11** was then obtained by conjugation with the carbohydrate derivative **A**[40,48] and unmasking of the hydroxyl groups gave the desired glycocluster **12**. As attested by the ^1H and ^{13}C NMR spectra, calixarenes **11** and **12** adopt the same flattened cone conformation. The two sets of signals observed for *t*Bu and Ar*H* confirm that **11** and **12** display a C_3 symmetry axis.[59] Moreover, the two well-defined doublets for the bridging methylene protons ($ArCH_2Ar$) indicate that the cone inversion does not occur on the NMR time scale. Finally in both cases, the methoxy protons display a drastic downfield shift with $\delta_{OMe} = 2.15$ and 2.19 ppm for **11** and **12**, respectively; this indicates that the three methoxy groups are oriented toward the centre of the cavity, while the three glycosylated arms are pointing outside of the calixarene core. In parallel, the per-propargylation of calix[6]arene **8** was also performed by using propargylbromide with sodium hydride as a base but the isolated yield of the hexapropargyl calix[6]arene **13** was only modest and not optimized. A better protocol for this process is now under investigation in our group. The CuAAC of the propargylated scaffold **13** with **A**[40,48] provided the desired glycoconjugate **14** and deprotection of the acetates afforded the hydroxylated hexavalent glycocluster **15**. In the case of the hexapropargylated calixarene **13**, only one signal is observed for *t*Bu ($\delta =$ 0.81 ppm), Ar*H* ($\delta = 7.15$ ppm) and the bridging methylene protons ($\delta \approx 4$ ppm). This data clearly indicates that compound **13** is flexible on the NMR time scale and also that the major conformation possesses a C_6 symmetry axis. Conversely, due to an increase of the bulkiness of the grafted arms, a loss of symmetry is observed for compounds **14** and **15** on the NMR time scale. Nevertheless, due to the high flexibility of those architectures, ^1H NMR spectra are broad and a mixture of several conformations is observed in both the cases.

Porphyrins are attractive scaffolds for the design of multivalent glycoconjugates particularly based on the potential applications of their intrinsic properties.[60–65] The synthesis of the tetrapropargylated porphyrin **17**[66,67] was performed from 4-propargyloxy-benzaldehyde (**16**)[68] (Scheme 3).

The subsequent CuAAC process systematically incorporated Cu^I in the non-metallated porphyrin **17** during the cycloaddition reaction leading to poor yields of cycloadducts or even complex mixtures of decomposed molecules. The NMR spectroscopic analyses of the mixtures obtained provided non-exploitable data due to the presence of copper ions in the porphyrin. We then tried a series of "click" chemistry conditions by using different sources of Cu^I for the conjugation of the non-metallated porphyrin **17** with the carbohydrate probe **A**[40,48] (Table 1). Since the metallation of the porphyrin was the main problem observed, we have selected triphenylphosphine–Cu^I complexes, which have been described recently to be more selective in CuAAC.[69] Both the bromide (available from commercial sources) and iodide[70] complexes were used, with or without microwave irradiation. Unfortunately, the partial incorporation of copper ions in the porphyrin's core was always observed and the non-metallated porphyrin could not be isolated under these conditions. The introduction of Zn^{2+} was, therefore, required prior to the "click" conjugation to obtain the desired Zn-metallated porphyrin **18**.[66,67] This metallation

 © 2011 Wiley-VCH Verlag GmbH & Co. KGaA, Weinheim

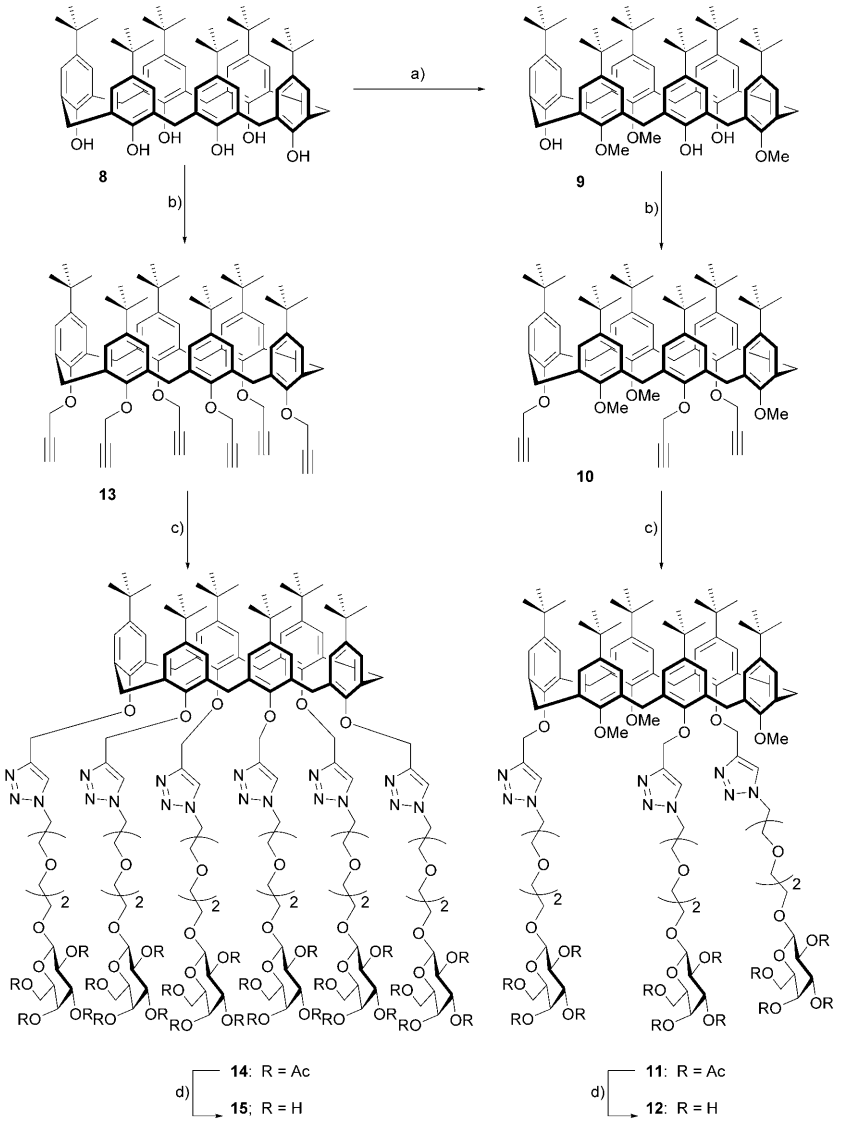

Scheme 2. a) MeI, K_2CO_3, acetone, reflux, 24 h, 35%; b) $HC\equiv CCH_2Br$, NaH, THF, reflux, 16 h, 87% for **9**, 18% for **13**; c) **A**, CuI, iPr_2NEt, DMF, μW, 110°C, 15 min, 65% for **11**, 84% for **14**; d) $MeOH/Et_3N/H_2O$ (5:1:1), RT, 4 days, 86% for **12**, 79% for **15**.

Table 1. Optimization of CuAAC conjugation of the propargylated non-metallated porphyrin **17** with the azido-functionalized carbohydrate derivative **A**.[a]

Cu^I catalyst	T [°C]	Activation	Observations
CuI	110	μW	metallation
$[CuBr(PPh_3)_3]$	110	μW	metallation
$[CuBr(PPh_3)_3]$	RT	none	metallation
$[CuI(PPh_3)_3]$	RT	none	metallation

[a] Conditions used: **17** (40 mg, 1 equiv), **A** (6 equiv), Cu^I catalyst (0.5 equiv), iPr_2NEt (5 equiv) in DMF (~5 mL).

process was optimised under microwave heating to reach fast and complete Zn^{2+} insertion. The CuAAC conjugation of the carbohydrate moiety then proceeded without transmetallation to afford the glycocluster **19** and was even compatible with the use of microwave heating. The acetylated glycoconjugate **19** was then deprotected to afford the desired glycocluster **20**.

Methyl β-D-galactopyranoside **22** and the triethyleneglycol-triazolyl **21**[24] were used as the monovalent references to determine the influence of the linker attached at the anomeric position, but also to study the importance of both valency and topology for each scaffold (Scheme 4). We have also recently synthesized two other tetravalent glycoclusters[24] based on a calix[4]arene core with two different locked topologies. The cone conformer **24** presents its four carbohydrate epitopes on one side of the calixarene rim (i.e. lower rim), whereas the 1,3-alternate conformer **23** displays two residues on each side of the ring. We have then studied the binding properties of the monovalent reference galactosides **21** and **22**, the five tetravalent glycoclusters **4**, **7**, **20**, **23** and **24** and also the hexavalent derivative **15** towards two galactose-binding lectins: PA-IL from *Pseudomonas aeruginosa* (PA-IL) and *Erythrina cristagalli* (ECA). The trivalent glycocluster **12** could not be included in this study due to its very poor solubility in water even with the addition of 5% DMSO.

Hemagglutination inhibition assays (HIA): A major interest of lectin-induced erythrocytes agglutination is probably that it reproduces the mode of binding of glycoconjugates to lectins in biological systems and is usually used as a rapid screening tool for multivalent glycoconjugates. Rabbit red cells hemagglutination by PA-IL and ECA was inhibited by the different glycoclusters synthesized above. The monovalent ligands **21** and **22** require millimolar range concentration for both lectins (Table 2). There is, therefore, almost no measurable influence of the linker arm based on HIA. The data measured for the multivalent glycoclusters will, therefore, account only for the valency and topology of these macromolecules.

The linear peptoid glycocluster **4** is not inhibiting hemagglutination with either ECA or PA-IL under the experimen-

 © 2011 Wiley-VCH Verlag GmbH & Co. KGaA, Weinheim

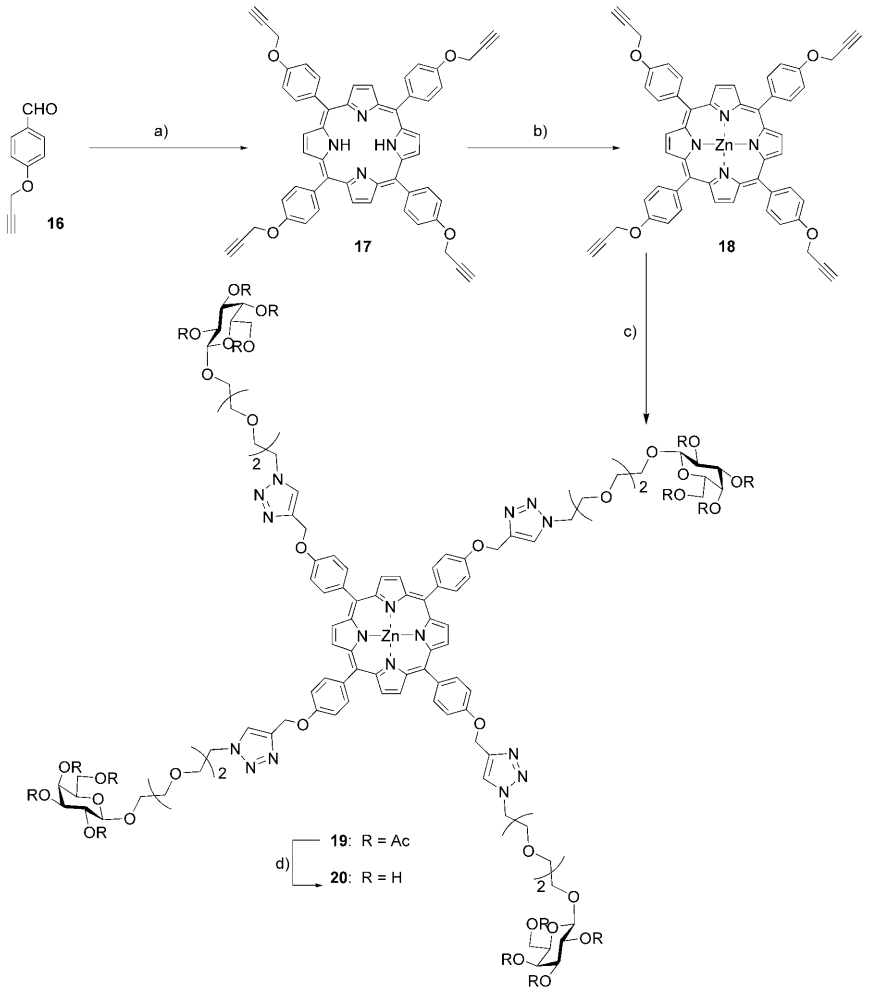

Scheme 3. a) $EtCO_2H$, pyrrole, 120 °C, 1 h, 23 %; b) $ZnCl_2$, Et_3N, μW, 120 °C, 15 min, 87 %; c) **A**, CuI, iPr_2NEt, DMF, μW, 110 °C, 15 min, 64 %; d) $MeOH/CH_2Cl_2/Et_3N/H_2O$ (5:1:1:1), RT, 4 days, 99 %.

Table 2. Hemagglutination inhibition assays for ECA and PA-IL.

Ligand	Valency	Minimum concentration[a] [μM]		Relative potency[b] [β]	
		ECA	PA-IL	ECA	PA-IL
21	1	2500	10000	1	1
22	1	5000	5000	0.5	2
4	4	>2500	>2000	nr[c]	nr[c]
7	4	625	>2000	4	nr[c]
20	4	1250	63	2	159
23	4	1160	500	2.1	20
24	4	2500	290	1	35
15	6	1250	63	2	159

[a] Minimum concentration required to inhibit the agglutination of erythrocytes. [b] Calculated as the ratio of the monovalent reference galactoside **21** value to the compound's value. [c] Not relevant.

tal conditions used. Nevertheless, its cyclic counterpart **7** displays a strong effect towards ECA while almost no binding was observed for PA-IL, which demonstrates selectivity related to the topology. The resulting potency is, however, too low to be described as an efficient "cluster effect".

On the opposite side, the porphyrin-based glycocluster **20** displays a clear preference for PA-IL versus ECA with a strong inhibition effect on the bacterial lectin. The relative potency observed for ECA is again very poor, but a much larger enhancement could be measured for PA-IL. The geometrical arrangement of the porphyrin scaffold is, therefore, much more appropriate to fit the spatial distribution of the multiple binding sites of PA-IL.

The tetravalent calix[4]arene-based glycoclusters **23** and **24** display only poor affinity towards ECA, at least in the same range as for the monovalent probes. Although their topology is very different from the porphyrin glycocluster **20**, the relative potency observed is still in the same range. When considering the binding properties of the glycoclusters **23** and **24** towards PA-IL, an improvement could be observed with inhibition in the micromolar range and a relative potency of roughly 30 for both molecules with a slight preference for the cone conformer **24**. While the topology of the calix[4]arene scaffold does not play a major role between 1,3-alternate and cone conformers, the square-planar topology of the porphyrin core is again much more suitable for a proper inhibition of PA-IL-induced hemagglutination.

The hexavalent glycocluster **15** displays the same inhibition properties as the tetravalent porphyrin-based molecule **20**, with a strong inhibition effect on PA-IL, and a weaker one on ECA. The inhibition is better than the one obtained with the calix[4]arenes **23** and **24**, which indicates that the higher valency is effective in increasing the affinity. However, this hexavalent compound is not better than the tetrameric one **20**. The square-planar topology of **20** is, therefore, more appropriate than the circular organization of the calix[6]arene derivative **15** in solution and a better affinity is measured towards PA-IL.

The HIA measurements display a selective binding profile for ECA and PA-IL. None of the compounds are really effective for binding ECA and few differences were observed between monovalent and multivalent ligand. While ECA does not select a strong ligand among the six glycoclusters studied, PA-IL displayed a much more contrasted selectivity

 © 2011 Wiley-VCH Verlag GmbH & Co. KGaA, Weinheim

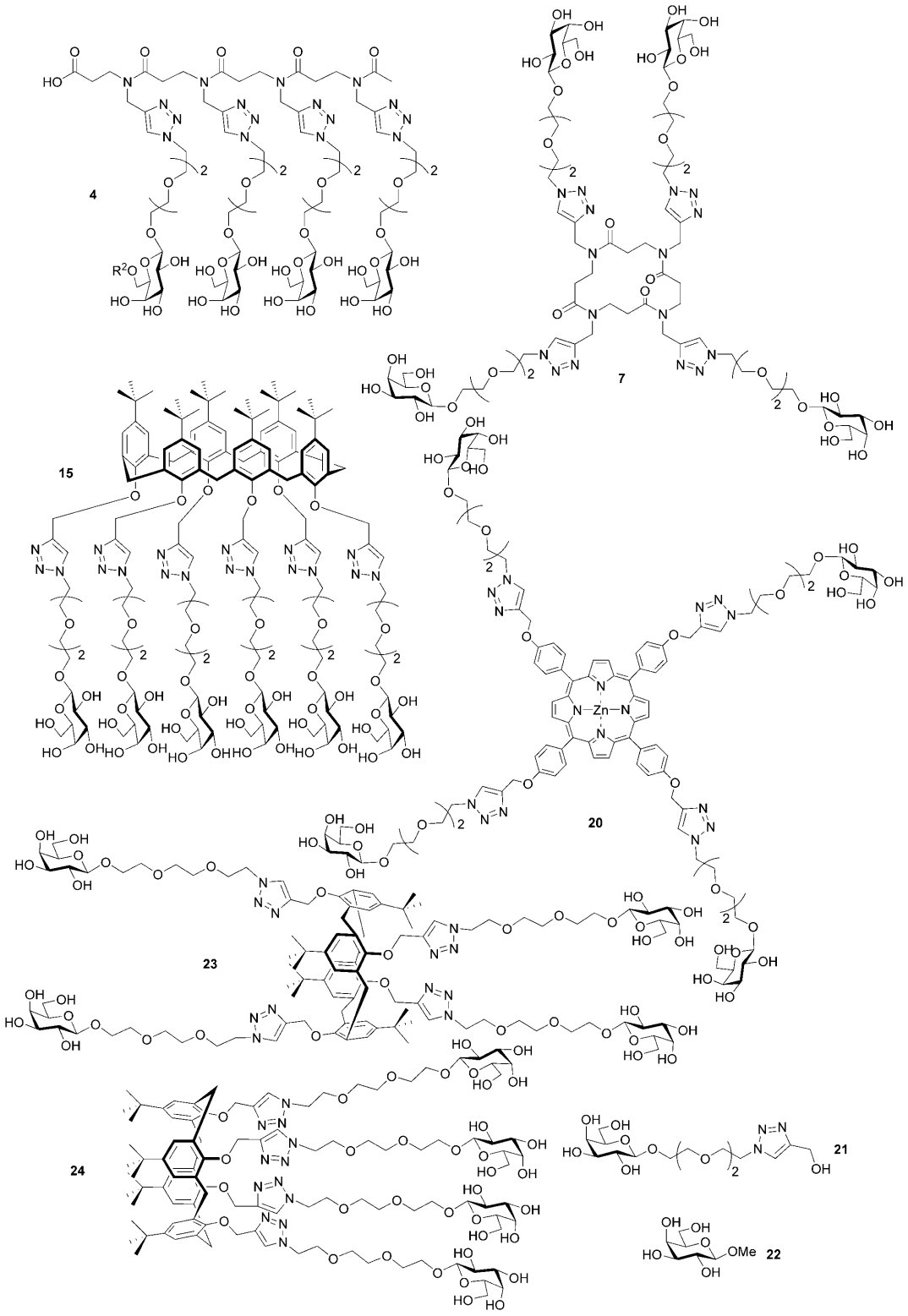

Scheme 4. Structure of the glycoclusters and their two monovalent reference ligands studied for their binding properties towards two galactose-binding lectins.

profile with a large preference for the porphyrin-based glycocluster **20** in comparison with the other tetravalent ligands.

Surface plasmon resonance (SPR): The SPR experiments were designed to mimic the inhibition of the lectin adhesion to a surface cell. A poly[*N*-(2-hydroxyethyl)acrylamide]

 © 2011 Wiley-VCH Verlag GmbH & Co. KGaA, Weinheim

polymer (PAA) presenting multiple α-galactose residues is attached by its biotin substituents to streptavidin-coated chips. The binding of PA-IL and ECA lectins is measured in the presence of increasing concentrations of glycoclusters, providing IC_{50} values (Table 3). The sensorgrams obtained with compound **15** and the inhibition curve are displayed in Figure 2. Data for all other compounds are provided in the Supporting Information (Figures S35–S43). The reference monovalent compound is the galactoside **21** displaying IC_{50} values in the micromolar range for both lectins.

Table 3. Inhibition of the adhesion of ECA and PA-IL to a surface covered with galactosides determined by SPR.

Ligand	Valency	IC_{50}[a] [μM]		Relative potency[b] [β]	
		ECA	PA-IL	ECA	PA-IL
21	1	210	63.5	1	1
4	4	11.5	3.5	18	18
7	4	41.6	2.5	5	25
20	4	26.6	1.4	8	45
23	4	nd[c]	0.9	nd[c]	70
24	4	nd[c]	1.4	nd[c]	45
15	6	5.2	0.8	40	80

[a] Minimum concentration of the inhibitor required to prevent 50% of the adhesion of the lectin onto the galactosylated surface of the SPR chip. [b] Calculated as the ratio of the monovalent reference galactoside **21** value to the compound's value. [c] Not determined.

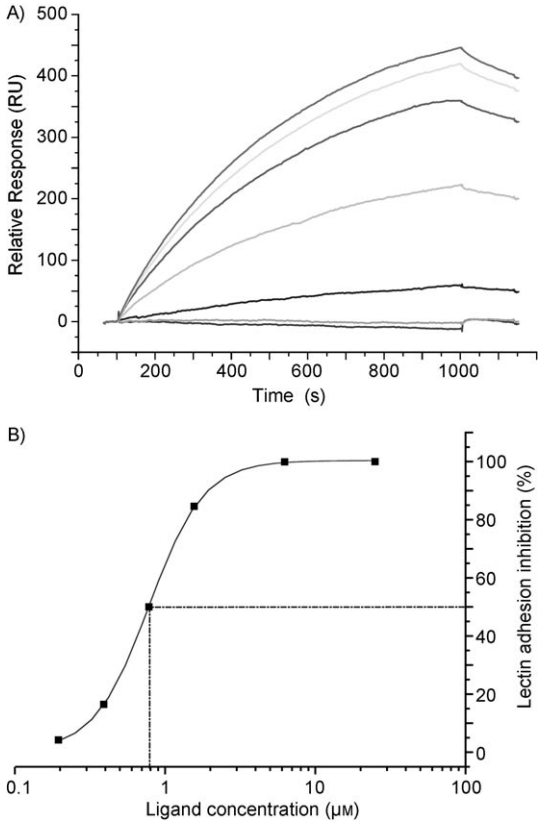

Figure 2. A) Sensorgrams obtained by injection of PA-IL incubated with concentrations of compound **15** varying from 0 μM (top curve) to 25 μM (bottom curve) on the PAA-α-D-galactose surface. B) Corresponding inhibition curve.

The cyclic peptoid glycocluster **7** displays weaker inhibition potency towards ECA in comparison to its linear analogue **4**. In contrast, no significant differences are observed for the binding of both compounds to PA-IL. These results are rather different from the one obtained by HIA experiments.

The porphyrin glycocluster **20** displays only a modest increase in binding towards ECA relative to the monovalent reference, whereas PA-IL displays a stronger preference for this topology. This observation confirms the HIA results, which indicates that the square-planar topology of this scaffold is very selective for the architecture of PA-IL.

The tetravalent calixarene glycoclusters were previously assayed[24] with SPR and the results reported here are in good agreement with the published ones considering variations in experimental conditions (e.g. equipment used, batch of lectin). Glycoclusters **23** and **24** display affinities in the low micromolar range towards PA-IL and the topology of the macromolecules is influential for the binding to the lectin, with the highest affinity observed for the 1,3-alternate conformer **23**. The best inhibitor for both lectins is the hexavalent calixarene glycocluster **15** displaying the highest relative potencies in comparison to the monovalent reference galactoside **21**.

The glycoclusters evaluated here by SPR display IC_{50} values in the micromolar to submicromolar range for both lectins (i.e. ECA and PA-IL). When considering the tetravalent glycoclusters, the influence of the topology of the molecules could always be detected and selectivity in binding between both lectins was also observed.

Isothermal titration microcalorimetry (ITC): Both HIA and SPR techniques demonstrated that the multivalent glycoclusters could result in important affinity improvements for PA-IL in comparison with ECA. Since PA-IL has been demonstrated to be a therapeutic target against lung infections by *Pseudomonas aeruginosa*,[71] an in-depth investigation has been performed by ITC to further characterize the interaction of PA-IL with the synthesized glycoclusters (Table 4). The thermogram and titration curve obtained with the hexavalent glycocluster **15** are displayed in Figure 3. Data for all other compounds are provided in the Supporting Information (Figures S30–S34).

The observed dissociation constants (K_d) of 70 μM for β-methyl-galactoside **22** and 150 μM for the compound with longer aglycon **21** are in the same range than the previously observed value of 50 μM for α-methyl-galactoside.[72]

The K_d value measured for the peptoid-based tetravalent glycoclusters **4** is in the low micromolar range. The change in scaffold from the linear compound **4** to the cyclic glycocluster **7** improves markedly the affinity towards PA-IL, with a resulting K_d of 296 nM. The cyclic spatial arrangement provides access to a fourth lectin monomer as depicted by the binding stoichiometry (n) value, which indicates a change from a 1:3 to a 1:4 glycocluster/lectin ratio for **4** and

 © 2011 Wiley-VCH Verlag GmbH & Co. KGaA, Weinheim

Table 4. Isothermal titration microcalorimetry (ITC) measurements for the glycoclusters and the monovalent probes **21** and **22** binding to PA-IL.[a]

Ligand	n[b]	$-\Delta H°$ [kJ mol^{-1}]	$-T\Delta S°$ [kJ mol^{-1}]	$-\Delta G°$ [kJ mol^{-1}]	K_d [μM]	Relative potency[c] [β]
21[d]	1[e]	36±1	14	22	150±1	1
22[f]	0.8[e]	39	15	24	70	2
4	0.33±0.02	87±11	54	33	1.8±0.4	83
7	0.18±0.01	176±4	139	37	0.30±0.03	500
20	0.46±0.04	60±7	23	37	0.33±0.06	454
23[d]	0.24±0.03	104±1	65	39	0.176±0.006	852
24[d]	0.33±0.01	71±6	34	37	0.42±0.16	357
15	0.32±0.01	85.9±0.6	47	39	0.14±0.01	1071

[a] Experiments have been duplicated and standard deviations are lower than 10% on stoichiometry and thermodynamic data and lower than 20% on dissociation constants. [b] Binding stoichiometry defined as the number of glycoclusters per monomer of PA-IL. [c] Calculated as the ratio of the monovalent reference galactoside **21** K_d value to the compound's K_d value. [d] Data from previous report.[24] [e] Value fixed during the fitting procedure. [f] Only one measurement performed.

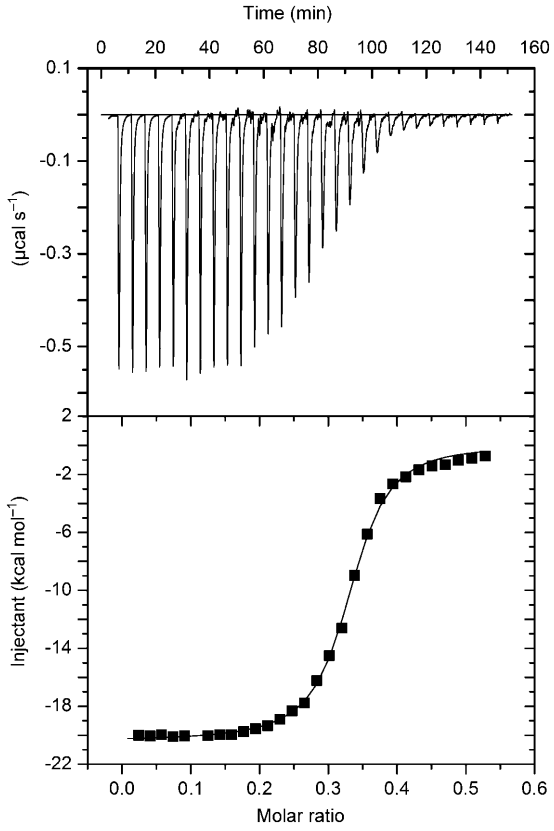

Figure 3. Raw ITC data obtained by injections of **15** (120 μM) in a solution containing PA-IL (50 μM; top). Corresponding integrated titration curve (bottom).

7, respectively. The stoichiometry of the complex formed between the tetravalent glycocluster **7** and the lectin could also be interpreted as a 1:5 complex, but this is rather improbable due to the four epitopes present on the glycocluster. Therefore, the n value of 0.18 measured for **7** is a little bit lower than the expected value of 0.25 for a typical 1:4 complex but can still be considered as a 1:4 complex due to structural features of the partners. The linear scaffold seems, therefore, to be more sterically constrained than its cyclic analogue, which can bind a lectin monomer on each of its four galactose residues. The effective "glycoside cluster effect" is also apparent in the thermodynamic of binding. Both compounds display strong enthalpy of binding, roughly proportional to the number of possible binding sites (as determined by stoichiometry n), with strong entropy barrier.

The porphyrin-based glycocluster **20** displays a high affinity with a K_d value of 332 nM associated to a stoichiometry value corresponding to the formation of a 1:2 complex with the lectin. The rigidity and the planar topology of this scaffold appears to be very favourable for lowering the entropy cost of binding, but this topology does not allow the attachment of one lectin monomer on each of the four galactose residues.

The hexavalent glycocluster **15** displays a K_d value of 136 nM, which makes it the highest affinity ligand identified to date for PA-IL. The binding process could be achieved through the formation of a chelate in which two binding sites of the lectin's tetramer are occupied by the carbohydrate epitopes and an additional "bind and jump" mode[73] (statistical rebinding) might also be implicated as at least one of the remaining four epitopes is still bound to a lectin monomer either from the same initial tetramer or from another lectin tetramer (Scheme 5). This process is a hypothesis based on the average 1:3 stoichiometry (n) of the complex measured by ITC and reflects the possible equilibrium between the different modes of binding implicating three

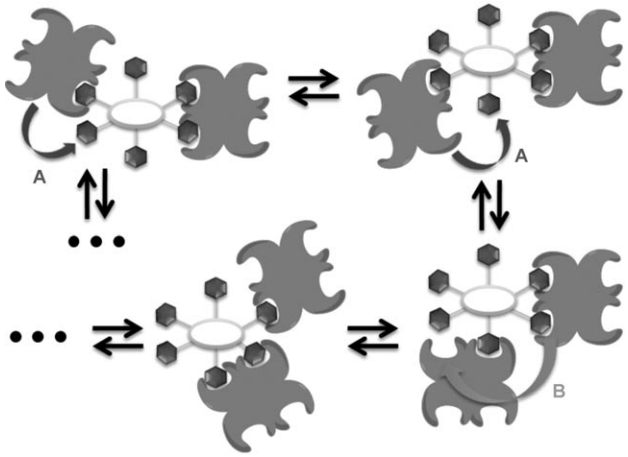

Scheme 5. Schematic representation of the possible binding modes between the hexavalent glycocluster **15** and PA-IL on the basis of a 1:3 stoichiometric ratio of glycocluster to lectin's monomer as determined by ITC. A) "Bind and jump" mechanism. B) Dissociation of one chelate and formation of another one.

 © 2011 Wiley-VCH Verlag GmbH & Co. KGaA, Weinheim

carbohydrate epitopes out of six of glycocluster **15**. The enthalpic contribution observed for the binding of **15** to PA-IL corresponds approximately to three monovalent binding events but the entropic cost is less important in comparison with other multivalent high affinity glycoclusters (e.g. **7** and **23**). The existence of multiple microstates and the "bind and jump" process[73] illustrated in Scheme 5 rationalize the fact that the entropy term does not vary proportionally with the number of binding events.

The data collected by ITC provide an interesting insight into the biomolecular interactions involved in solution between synthetic glycoclusters and PA-IL. The geometry of the macromolecules influences the binding to the lectin not only in terms of dissociation constant values and thermodynamic patterns but also in the stoichiometric ratio with the protein.

Comparison of HIA, SPR and ITC results: This work also illustrates the differences that can be observed when comparing binding data obtained from solution experiments (ITC), surface adhesion (SPR) or aggregation (HIA). Some of the high affinity compounds in solution (i.e. the peptoid compounds **4** and **7**) remain medium-range inhibitors of surface binding and very poor ones against hemagglutination. In this case, the conjugated effect of multivalency and high flexibility can be the cause of this failure. Indeed, multivalent compounds, instead of inhibiting the binding of the lectin to the surface of chips, have the properties to establish a complex tridimensional network cross-linking surface–lectin–ligand–lectin. This would result in recruiting more lectins to the surface, which is actually the opposite of the desired effect. Interestingly, not all multivalent molecules presented this bias, and two compounds, namely **15** and **20**, are excellent inhibitors in all experimental setups. Multivalent interactions can proceed through several mechanisms (chelate, aggregative, aggregative chelate, statistical rebinding) that are inherently concentration-dependant. Different experimental techniques measure different processes.[4,74] HIA, SPR and ITC methodologies intrinsically generate variations in local analyte concentrations thus influencing equilibria in which a particular binding mechanism would be favoured compared to others. This clearly illustrates the requirement of multiple synthetic approaches and experimental analyses of multivalent interactions for the design of high-affinity multivalent ligands that could efficiently inhibit lectin binding.

Conclusion

The design of multivalent glycoconjugates as high-affinity ligands of lectins is the source of both fundamental and potential applied research particularly for the development of new anti-infective agents. The better understanding of the multivalent lectin–carbohydrate interactions is crucial in this field and requires the design of several synthetic multivalent molecular architectures incorporating a large set of core scaffolds, linker arms and carbohydrate epitopes. The synthesis of five tetravalent glycoclusters incorporating a linear and a cyclic peptoid scaffold, calix[4]arenes and a porphyrin was achieved by 1,3-dipolar cycloaddition between the propargylated cores and an azido-functionalized galactoside. Similarly, an hexavalent glycocluster was prepared from the corresponding hexapropargylated calix[6]arene. The detailed analysis of the binding properties of each multivalent ligand with two lectins (ECA and PA-IL) was performed by HIA, SPR and ITC. The influence of the geometry of the central scaffold could be observed particularly from the linear to cyclic glycoclusters. The HIA and SPR analyses could illustrate the selectivity of each ligand for either ECA or PA-IL with sometimes large differences in the affinities measured. This selectivity observed in vitro implies that topology-induced selectivity in natural multivalent binding in vivo might be of prime importance. The calix[6]arene-based hexavalent glycocluster displayed the best binding properties. These molecules are, therefore, candidates for the design of anti-infective agents and more particularly for the development of antibacterial treatments against infection by *Pseudomonas aeruginosa*.

Experimental Section

General methods: All reagents for synthesis were commercial and used without further purification. Solvents were distilled over CaH_2 (CH_2Cl_2), Mg/I_2 (MeOH), Na/benzophenone (THF) or purchased dry. All reactions were performed under an argon atmosphere. Reactions under microwave activation were performed on a Biotage Initiator system. NMR spectra were recorded at 293 K, unless otherwise stated, by using a 300 or 400 MHz spectrometer. Shifts are referenced relative to deuterated solvent residual peaks. The following abbreviations are used to explain the observed multiplicities: s, singlet; d, doublet; t, triplet; q, quadruplet; m, multiplet and brs, broad singlet. Due to the high conformational flexibility of the peptoid and calixarene backbones, some signals are missing in the ^1H and/or ^{13}C spectra (e.g. carbonyl, C-triazole, CH_2-peptoid and N–CH_2-triazole). This conformational flexibility could also be observed in proton spectra as some proton signals are broadened. However, correlation traces were observed in 2D experiments (HSQC and HMBC) and assignments were deduced from these 2D correlation spots. Melting points are reported uncorrected. IR spectra were recorded by using an FTIR spectrometer with ATR attachment. High-resolution (LSIMS) mass spectra were recorded in the positive mode by using a Thermo Finnigan Mat 95 XL spectrometer. ESI mass spectra were recorded in the positive mode by using a Thermo Finnigan LCQ spectrometer. High-resolution (HR-ESI-QTOF) mass spectra were recorded by using a Bruker MicrOTOF-Q II XL spectrometer. MALDI-ToF mass spectra were recorded in positive-ion reflectron mode by using a Voyager DE-STR spectrometer (Applied Biosystem) with CHCA (ϕ-cyano-4-hydroxycinnamic acid, 10 g L^{-1} in MeOH) and NaI (10 g. L^{-1} in acetone) as the matrix. TLC was carried out on aluminium sheets coated with silica gel 60 F_{254} (Merck). TLC plates were inspected by UV light ($\lambda = 254$ nm) and developed by treatment with a mixture of 10% H_2SO_4 in EtOH/H_2O (95:5 v/v) followed by heating. Silica gel column chromatography was performed with silica gel Si 60 (40–63 μm). Optical rotation was measured by using a Perkin–Elmer polarimeter and values are given in 10^{-1} deg cm^2 g^{-1}. The following conditions were used for the synthesis and analyses of **2**. IR spectra were recorded on a Shimadzu FTIR-8400S IR spectrophotometer and ν are expressed in cm^{-1}. NMR spectra were recorded on a Bruker AC 400 spectrometer (^1H at 400 MHz, ^{13}C at 100 MHz). HRMS were recorded in electrospray ionization mode on a micro q-tof Micromass in-

 © 2011 Wiley-VCH Verlag GmbH & Co. KGaA, Weinheim

strument (3000 V) with an internal lock mass (H_3PO_4) and an external lock mass (Leu-enkephaline). Lyophilized ECA was purchased from Sigma–Aldrich. Recombinant PA-IL was produced in *E. coli* and ITC measurements were performed according to our previously reported protocols.[24]

General procedure for 1,3-dipolar cycloadditions (method A): The alkyne-functionalized scaffold, copper iodide, *i*Pr_2Net and azido-functionalized galactoside **A** in degassed DMF were introduced in a Biotage Initiator 2–5 mL vial. The vial was flushed with argon and protected from light (aluminium sheet) and the solution was sonicated for 30 s. The vial was sealed with a septum cap and heated at 110 °C under microwave irradiation (solvent absorption level: high). After uncapping the vial, the crude mixture was diluted with EtOAc (200 mL). The organic layer was washed with HCl (1 N, 2×50 mL), water (4×50 mL) and brine (50 mL) unless otherwise stated. The organic layer was dried (Na_2SO_4), filtered and evaporated. The crude product was purified by flash silica gel column chromatography to afford the desired acetylated glycoclusters.

General procedure for deacetylation of glycoclusters (method B): The acetylated glycocluster was suspended in distilled MeOH, ultra-pure water and ultra-pure triethylamine (5:1:1, v/v/v) unless otherwise stated. The mixture was stirred under argon at room temperature for 3 to 4 days. Solvents were evaporated, co-evaporated with toluene and the residue was dissolved in ultra-pure water (5 mL) and then freeze-dried to afford the pure glycocluster without further purification.

***tert*-Butyl (4,8,12,16-tetra-aza)(5,9,13,17-tetra-oxo)(4,8,12,16-tetra-*N*-propargyl)octadecanoate (2)**: Acetic anhydride (717 μL, 7.63 mmol, 10 equiv) was added to a solution of amine **1** (390 mg, 0.76 mmol) in CH_2Cl_2 (25 mL). The mixture was stirred at RT over 5 h and then concentrated under reduced pressure. The crude mixture was diluted with AcOEt (20 mL) and then washed with a saturated solution of $NaHCO_3$ (2×10 mL), a solution of $KHSO_4$ (5%; 2×10 mL) and then brine (10 mL). The organic layer was dried ($MgSO_4$), filtered and then concentrated under reduce pressure. Purification by flash chromatography (AcOEt/MeOH 95:5) provided compound **2** as a pale-yellow oil (408 mg, 97%). R_f=0.25 (EtOAc); ^{1}H NMR (400 MHz, $CDCl_3$): δ=4.11–4.23 (m, 8H), 3.63–3.84 (m, 8H), 2.75–2.90 (m, 6H), 2.52–2.60 (m, 2H), 2.27–2.34 (m, 2H), 2.22 (m, 2H), 2.19 (s, 3H), 2.16, 2.15 1.44 ppm (s, 9H); ^{13}C NMR (100 MHz, $CDCl_3$): δ=173.7 (C), 171.4 (4C), 170.9, 170.8, 170.3, 170.1, 170.0, 169.7, 81.4 (C), 81.2, 80.7, 79.1 (4C), 78.6, 78.4, 73.0 (4CH), 72.8, 72.5, 72.0, 71.8, 44.2 (4×CH_2), 44.0, 43.7, 43.5, 43.4, 43.3, 43.2, 43.1, 42.8, 42.6, 39.7 (2×CH_2), 39.6, 38.8, 38.7, 38.6, 38.3, 38.2, 34.6 (3×CH_2), 34.3, 34.1, 33.9, 33.8, 31.9 (3×CH_2), 31.8, 31.7, 31.6, 31.5, 31.4, 27.9 (3CH_3), 21.2 (CH_3), 20.6 ppm; IR (neat): νÜ=>=1153, 1367, 1417, 1641, 1722, 2120, 2935, 2976, 3246, 3290 cm^{-1}; HR-ESI-MS: *m*/*z*: calcd for $C_{30}H_{41}N_4O_6$: 553.3026 $[M+H]^+$; found: 553.3034.

***tert*-Butyl (4,8,12,16-tetra-*N*-{1-[(2,3,4,6-tetra-*O*-acetyl-β-D-galactopyranosyloxy)-3,6-dioxaoct-8-yl]-1,2,3-triazol-4-yl}-4-methyl)(4,8,12,16-tetra-aza)(5,9,13,17-tetra-oxo)octadecanoate (3)**: Obtained as a colourless gum (464 mg, 86%) by following method A: **2** (116 mg, 0.21 mmol, 1 equiv), **A** (586 mg, 1.16 mmol, 5.5 equiv), CuI (20 mg, 0.11 mmol, 0.5 equiv) and *i*Pr_2NEt (183 μL, 1.05 mmol, 5 equiv) in DMF (3 mL). Microwave irradiation: 15 min at 110 °C. After dilution of the crude mixture in EtOAc (300 mL), the organic layer was washed by NH_4Cl (2×150 mL) and water (2×150 mL). The residue was purified by Al_2O_3 gel flash chromatography (EtOAc then EtOAc/MeOH 4:1). R_f=0.53 (EtOAc/MeOH 95:5); $[\alpha]_D$=−4.7 (c=1.10 in CH_2Cl_2); ^{1}H NMR (300 MHz, $CDCl_3$): δ=7.85–7.61 (m, 4H; H-triaz), 5.37 (dd, J=3.2, <1 Hz, 4H; H-4), 5.18 (dd, J=10.4, 8.0 Hz, 4H; H-2), 5.02 (dd, J=10.4, 3.2 Hz, 4H; H-3), 4.66–4.42 (m, 20H; H-1, NCH_2C-triaz, OCH$_2$CH_2N-triaz), 4.21–4.05 (m, 8H; H-6a, H-6b), 4.00–3.79 (m, 16H; H-5, 1/2 GalOCH_2CH$_2$O, 1×CH_2-EG$_3$), 3.76–3.66 (m, 8H; 1/2 GalOCH_2CH$_2$O, 2×CH_2-peptoid), 3.66–3.52 (m, 28H; 3×CH_2-EG$_3$, 2×CH_2-peptoid), 2.97–2.42 (m, 8H; 4×CH_2-peptoid), 2.13, 2.03, 1.97 (3 s, 4×12H; CH_3CO), 1.84 (s, 3H; CH_3), 1.41 ppm (br s, 9H; *t*Bu); ^{13}C NMR (75 MHz, $CDCl_3$): δ=170.5, 170.4, 170.3, 169.6 (4 s; 4×CH_3CO), 101.5 (C-1), 71.0 (C-3), 70.8 (C-5), 70.8, 70.7, 70.3, 69.5 (4 s; $CH_2OCH_2CH_2OCH_2$), 69.3 (GalOCH_2), 68.9 (C-2), 67.2 (C-4), 61.4 (C-6), 50.4 (OCH$_2$CH_2N-triaz), 28.2 (CMe_3), 20.9, 20.8, 20.7 ppm (3 s; 4×CH_3CO, CH_3); HR-LSIMS-MS: *m*/*z*: calcd for $C_{110}H_{165}N_{16}O_{54}$: 2574.0657 $[M+H]^+$; found: 2574.0697.

(4,8,12,16-Tetra-aza)(4,8,12,16-tetra-*N*-{1-[(β-D-galactopyranosyloxy)-3,6-dioxaoct-8-yl]-1,2,3-triazol-4-yl}-4-methyl)(5,9,13,17-tetra-oxo)octadecanoic acid (4): Obtained as a freeze-dried white solid (109 mg, 77%) by following a variation of method B: Compound **3** (198 mg, 77 μmol, 1 equiv) was suspended in THF (5 mL) and aqueous NaOH (4 M, 5 mL). After stirring at RT for 16 h, the reaction mixture was neutralized by using Amberlite IR-120 H^+ resin until pH 5 was obtained. After filtration, washing (MeOH) and concentration, the product was dissolved in water (5 mL) and then freeze-dried to afford the pure deacetylated glycocluster **4**. $[\alpha]_D$=+3.1 (c=0.45 in H_2O); ^{1}H NMR (300 MHz, CD_3OD): δ=8.19–7.86 (m, 4H; H-triaz), 4.78–4.50 (m, 16H; NCH_2C-triaz, OCH$_2$CH_2N-triaz), 4.29 (d, J=6.3 Hz, 4H; H-1), 4.05–3.81 (m, 16H; H-4, 1/2 GalOCH_2CH$_2$O, OCH_2CH$_2$N-triaz), 3.79–3.69 (m, 16H; H-6a, H-6b, 1/2 GalOCH_2CH$_2$O, 2×CH_2-peptoid), 3.61 (br s, 28H; 3×CH_2-EG$_3$, 2×CH_2-peptoïd), 3.57–3.42 (m, 12H; H-2, H-3, H-5), 3.04–2.47 (m, 8H; 4×CH_2-peptoïd), 2.29–2.14 ppm (m, 3H; CH_3); ^{13}C NMR (75 MHz, CD_3OD): δ=173.8, 173.5 (2 s, 4C; O=C-peptoid), 144.8 (C^{IV}-triaz), 125.5 (CH-triaz), 104.9 (C-1), 76.6, 74.8, 72.5 (C-2, C-3, C-5), 71.3 (3×CH_2-EG$_3$), 70.3 (1 s; C-4, OCH_2CH$_2$N-triaz), 69.6 (GalOCH_2-), 62.5 (C-6), 51.4 (OCH$_2$CH_2N-triaz), 21.2, 21.7 ppm (CH_3, 2 conformers); HR-ESI-QTOF MS (positive mode) *m*/*z*: calcd for $C_{74}H_{124}N_{16}NaO_{38}$: 1867.8155 $[M+Na]^+$; found: 1867.8181; calcd for $C_{74}H_{124}N_{16}Na_2O_{38}$: 945.4023 $[M+2Na]^{2+}$; found: 945.4056.

(4,8,12,16-Tetra-*N*-{1-[(2,3,4,6-tetra-*O*-acetyl-β-D-galactopyranosyloxy)-3,6-dioxaoct-8-yl]-1,2,3-triazol-4-yl}-4-methyl)(4,8,12,16-tetra-aza)(1,5,9,13-tetra-oxo)cyclohexadecane (6): Obtained as a white foam (166 mg, 77%) by following method A: Compound **5** (38 mg, 87 μmol, 1 equiv), **A** (264 mg, 0.522 mmol, 6 equiv), CuI (8 mg, 0.5 equiv) and *i*Pr_2NEt (56 μL, 5 equiv) in DMF (3 mL). Microwave irradiation: 30 min at 110 °C. After concentration of the crude mixture and three co-evaporations with toluene, the residue was purified by Al_2O_3 flash chromatography (EtOAc then EtOAc/MeOH 85:15). R_f=0.15 (EtOAc/MeOH 4:1); $[\alpha]_D$=−3.5 (c=0.92 in CH_2Cl_2); ^{1}H NMR (300 MHz, $CDCl_3$): δ=7.72–7.55 (m, 4H; H-triaz), 5.34 (d, J=3.1 Hz, 4H; H-4), 5.19–5.10 (m, 4H; H-2), 4.99 (dd, J=10.4, 3.1 Hz, 4H; H-3), 4.63–4.41 (m, 20H; H-1, OCH$_2$CH_2N-triaz, NCH_2C-triaz), 4.18–4.06 (m, 8H; H-6a, H-6b), 3.98–3.88 (m, 8H; H-5, 1/2 GalOCH_2CH$_2$O), 3.87–3.79 (m, 8H; OCH_2CH$_2$N-triaz), 3.78–3.62 (m, 12H; 1/2 GalOCH_2CH$_2$O, NC(O)CH_2CH$_2$N), 3.60–3.52 (m, 24H; 3×CH_2-EG$_3$), 2.88–2.57 (m, 8H; NC(O)CH$_2$CH_2N), 2.10, 2.00, 1.94 ppm (3 s, 4×12H; CH_3CO); ^{13}C NMR (100 MHz, $CDCl_3$): δ=172.0, 171.1, 170.5, 170.4, 170.3, 170.2, 170.1, 169.5 (8 s, 8C; C=O), 144.2, 144.1, 143.9, 143.7 (4 s, 4C; C^{IV}-triaz), 124.4, 124.2, 123.6, 122.7 (4 s, 4C; CH-triaz), 101.4 (C-1), 70.9 (C-3), 70.7 (C-5), 70.6, 70.5, 70.2 (3×CH_2-EG$_3$), 69.5 (OCH_2CH$_2$N-triaz), 69.2 (GalOCH_2-), 68.9 (C-2), 67.1 (C-4), 61.3 (C-6), 50.2 (OCH$_2$CH_2N-triaz), 45.4, 45.3, 44.9, 44.5, 42.5, 41.3, 40.5 (7 s, 8C; NCH_2C-triaz, NC(O)CH_2CH$_2$N), 32.4, 31.8 (2 s, 4C; NC(O)CH$_2$CH_2N), 28.2 ((CH_3)$_3$C-), 20.8, 20.7, 20.7 ppm (3 s, 4×CH_3CO; CH_3); HR-MALDI-TOF MS (positive-ion reflectron mode): *m*/*z*: calcd for $C_{104}H_{152}N_{16}NaO_{52}$: 2479.9636; found: 2479.9638.

(4,8,12,16-Tetra-aza)(4,8,12,16-tetra-*N*-{1-[(β-D-galactopyranosyloxy)-3,6-dioxaoct-8-yl]-1,2,3-triazol-4-yl}-4-methyl)(1,5,9,13-tetra-oxo)cyclohexadecane (7): Obtained as a freeze-dried white solid (97 mg, 87%) by following method B: Compound **6** (160 mg, 62 μmol, 1 equiv) was suspended in methanol (2 mL), water (0.5 mL) and triethylamine (0.5 mL). After stirring at RT for 4 days and concentration, the mixture was co-evaporated with toluene three times, dissolved in ultra-pure water (4 mL) and freeze-dried to afford the pure deacetylated glycocluster. $[\alpha]_D$=+0.6 (c=0.95 in H_2O); ^{1}H NMR (400 MHz, DMSO+traces CD_3OD): δ=8.11–7.83 (m, 4H; H-triaz), 4.54–4.41 (m, 16H; NCH_2C-triaz, OCH$_2$CH_2N-triaz), 4.13–4.04 (m, 4H; H-1), 3.86–3.72 (m, 12H; 1/2 GalOCH_2CH$_2$O, OCH_2CH$_2$N-triaz), 3.62–3.58 (m, 4H; H-4), 3.57–3.40 (m, 36H; 1/2 GalOCH_2CH$_2$O, H-6a, H-6b, 3×CH_2-EG$_3$), 3.35–3.28 (m, 4H; H-5), 3.28–3.21 ppm (m, 8H; H-2, H-3); ^{13}C NMR (100 MHz, DMSO+traces CD_3OD): δ=173.3, 170.4 (2 s, 4C; O=C-peptoid), 143.9 (C^{IV}-triaz), 124.1 (CH-triaz), 103.7 (C-1), 75.4 (C-5), 73.5, 70.7 (2 s, 8C; C-2, C-3), 70.0, 69.9, 69.8 (3×CH_2-EG$_3$), 68.9 (OCH$_2$CH$_2$N-triaz), 68.4 (C-4), 68.1

 © 2011 Wiley-VCH Verlag GmbH & Co. KGaA, Weinheim

(GalOCH_2-), 60.7 (C-6), 49.7 (OCH_2CH_2N-triaz), 39.5 ppm* (NCH_2C-triaz; signal partially overlapped by residual $CHCl_3$ peak); HR-MALDI-TOF MS (positive-ion reflectron mode): *m/z*: calcd for $C_{72}H_{120}N_{16}NaO_{36}$: 1807.7947 $[M+Na]^+$; found: 1807.8008.

5,11,17,23,29,35-Hexa-*tert*-butyl-38,40,42-tri-({1-[(2,3,4,6-tetra-*O*-acetyl-β-D-galactopyranosyloxy)-3,6-dioxaoct-8-yl]-1,2,3-triazol-4-yl}-4-methyleneoxy)-37,39,41-trimethoxy-calix[6]arene (11): Obtained as a pale-yellow foam (79 mg, 65%) by following method A: Compound **10**[58] (52 mg, 46 μmol, 1 equiv), **A** (105 mg, 0.210 mmol, 4.5 equiv), CuI (4.4 mg, 23 μmol, 0.5 equiv) and *i*Pr_2NEt (40 μL, 0.23 mmol, 5 equiv) in DMF (3 mL). Microwave irradiation: 15 min at 110 °C. After workup, the residue was purified by silica gel flash chromatography (EtOAc then EtOAc/MeOH 9:1). R_f = 0.73 (EtOAc/MeOH 9:1); $[\alpha]_D$ = −4.6 (c = 0.57 in CH_2Cl_2); ^{1}H NMR (300 MHz, $CDCl_3$): δ = 7.90 (s, 3H; H-triaz), 7.26 (s, 6H; H-ar), 6.64 (s, 6H; H-ar), 5.35 (d, J = 3.3 Hz, 3H; H-4), 5.17 (dd, J = 10.4, 7.9 Hz, 3H; H-2), 5.08 (s, 6H; OCH_2C-triaz), 4.99 (dd, J = 10.4, 3.3 Hz, 3H; H-3), 4.61–4.47 (m, 15H; H-1, Ar-CH_2-Ar, OCH_2CH_2N-triaz), 4.18–4.02 (m, 6H; H-6a, H-6b), 3.90 (m, 12H; 1/2 GalOCH_2CH_2O, H-5, OCH_2CH_2N-triaz), 3.72–3.63 (m, 3H; 1/2 GalOCH_2CH_2O), 3.60–3.46 (m, 18H; 3×CH_2-EG$_3$), 3.34 (d, J = 15.1 Hz, 6H; Ar-CH_2-Ar), 2.15 (s, 9H; OCH_3), 2.12, 2.01, 2.00, 1.95 (4 s, 4×9H; 4×CH_3CO), 1.36 (s, 27H; 3×CMe_3), 0.78 ppm (s, 27H; 3×CMe_3); ^{13}C NMR (75 MHz, $CDCl_3$): δ = 170.5, 170.3, 170.2, 169.5 (4 s; CH_3CO), 154.4 (C^{IV}-ar), 151.6 (C^{IV}-ar), 146.2 (C^{IV}-C$(CH_3)_3$), 145.0 (C^{IV}-C$(CH_3)_3$), 144.7 (C^{IV}-triaz), 133.7 (C^{IV}-OMe), 133.0 (C^{IV}-OMe), 128.2 (CH-ar), 124.1 (CH-triaz), 123.7 (CH-ar), 101.4 (C-1), 71.0 (C-3), 70.70 (C-5), 70.68 (2×CH_2-EG$_3$), 70.3 (1×CH_2-EG$_3$), 69.6 (GalOCH_2-), 69.2 (OCH_2CH_2N-triaz), 68.9 (C-2), 67.2 (C-4), 66.5 (OCH_2C-triaz), 61.3 (C-6), 60.2 (OCH_3), 50.3 (OCH_2CH_2N-triaz), 34.3 (CMe_3), 34.0 (CMe_3), 31.7 (CMe_3), 31.2 (CMe_3), 28.8 (Ar-CH_2-Ar), 20.9, 20.8, 20.7 ppm (3 s, 12C; 12×CH_3CO); HR-MALDI-TOF MS (positive-ion reflectron mode): *m/z*: calcd for $C_{138}H_{189}N_9NaO_{42}$: 2667.2825 $[M+Na]^+$; found: 2667.2908.

5,11,17,23,29,35-Hexa-*tert*-butyl-38,40,42-tri({1-[(β-D-galactopyranosyloxy)-3,6-dioxaoct-8-yl]-1,2,3-triazol-4-yl}-4-methyleneoxy)-37,39,41-trimethoxy-calix[6]arene (12): Obtained as a freeze-dried white solid (55 mg, 86%) by following method B: Compound **11** (79 mg, 30 μmol) was suspended in methanol (15 mL), water (3 mL) and triethylamine (3 mL). After stirring at RT for 3 days and concentration, the mixture was dissolved in ultra-pure water (4 mL) and then freeze-dried to afford the pure deacetylated glycocluster. $[\alpha]_D$ = −2.8 (c = 0.32 in DMSO); ^{1}H NMR (300 MHz, CD_3OD): δ = 8.29 (s, 3H; H-triaz), 7.32 (s, 6H; H-ar), 6.72 (s, 6H; H-ar), 5.11 (s, 6H; OCH_2C-triaz), 4.70–4.61 (m, 6H; OCH_2CH_2N-triaz), 4.53 (d, J = 15.7 Hz, 6H; Ar-CH_2-Ar), 4.23 (d, J = 7.4 Hz, 3H; H-1), 4.01–3.87 (m, 6H; OCH_2CH_2N-triaz), 3.81 (d, J = 2.4 Hz, 3H; H-4), 3.78–3.62 (m, 9H; H-6a, H-6b, GalOCH_2-), 3.62–3.38 (m, 27H; H-2, H-3, H-5, 3×CH_2-EG$_3$), 3.28–3.22 (m, 6H; Ar-CH_2-Ar), 2.19 (s, 9H; OCH_3), 1.40 (s, 27H; 3×CMe_3), 0.80 ppm (s, 27H; 3×CMe_3); ^{13}C NMR (75 MHz, CD_3OD): δ = 155.5 (C^{IV}-ar), 152.7 (C^{IV}-ar), 147.2 (C^{IV}-ar), 147.2 (C^{IV}-ar), 145.4 (C^{IV}-triaz), 135.1 (C^{IV}-OMe), 134.4 (C^{IV}-OMe), 129.4 (CH-ar), 126.9 (CH-triaz), 124.9 (CH-ar), 105.1 (C-1), 76.6, 74.9, 72.5 (C-2, C-3, C-5), 71.5, 71.4 (2 s; 6C, 2×CH_2-EG$_3$), 70.5 (OCH_2CH_2N-triaz), 70.3 (C-4), 69.6 (1×CH_2-EG$_3$), 68.8 (GalOCH_2-), 66.9 (OCH_2C-triaz), 62.5 (C-6), 61.3 (OCH_3), 51.5 (OCH_2CH_2N-triaz), 35.2 (CMe_3), 35.1 (CMe_3), 32.1 (CMe_3), 31.9 (CMe_3), 30.7 ppm (Ar-CH_2-Ar); HR-ESI-QTOF MS (positive mode): *m/z*: calcd for $C_{114}H_{165}N_9NaO_{30}$: 2163.1560 $[M+Na]^+$; found: 2163.1568.

5,11,17,23,29,35-Hexa-*tert*-butyl-37,38,39,40,41,42-hexapropargyloxy-calix[6]arene (13): Calix[6]arene **8**[56] (1.77 g, 1.90 mmol) was added to a solution of NaH (60 wt.% in oil, 1.307 g, 32.7 mmol, 17 equiv) in anhydrous THF (50 mL). The reaction mixture was refluxed for 30 min and then propargyl bromide (3.49 mL, 30.1 mmol, 16 equiv) was added dropwise. After 15 h of refluxing, the reaction mixture was concentrated to 1/3 of the initial volume and HCl (1 M, 50 mL) was carefully added at 0 °C. The organic layer was then extracted with chloroform (3×30 mL), washed with saturated NH_4Cl (2×30 mL), dried (Na_2SO_4), filtered and concentrated under reduce pressure. The crude residue was triturated in diethylether and then filtered, giving pure compound **13** (401 mg, 18%) as a slightly pale-yellow solid. M.p. 220 °C dec; IR (KBr): $\tilde{\nu}$ = 3288, 2953, 1719, 1478, 1362, 1188, 1113, 1004, 875 cm^{-1}; ^{1}H NMR (300 MHz, $CDCl_3$): δ = 7.15 (s, 12H; H-ar), 3.87–4.15 (m, 24H; ArCH_2 OCH_2), 1.28 (s, 6H; C≡CH), 0.81 ppm (s, 54H; CMe_3); ^{13}C NMR (75 MHz, $CDCl_3$): δ = 153.3, 146.4, 133.4, 126.6 (ArC), 79.7 (C≡CH), 75.3 (OCH_2), 61.1 (C≡CH), 34.5 (ArCH_2), 31.6 ppm (CMe_3); HR-ESI-QTOF MS: *m/z*: calcd for $C_{84}H_{96}NaO_6$: 1223.7105 $[M+Na]^+$; found: 1223.7045.

5,11,17,23,29,35-Hexa-*tert*-butyl-37,38,39,40,41,42-hexa-({1-[(2,3,4,6-tetra-*O*-acetyl-β-D-galactopyranosyloxy)-3,6-dioxaoct-8-yl]-1,2,3-triazol-4-yl}-4-methyleneoxy)calix[6]arene (14): Obtained as a pale-yellow foam (153 mg, 84%) by following method A: Compound **13** (52 mg, 43 μmol, 1 equiv), **A** (196 mg, 0.390 mmol, 9 equiv), CuI (4 mg, 22 μmol, 0.5 equiv) and *i*Pr_2NEt (40 μL, 0.21 mmol, 5 equiv) in DMF (3 mL). Microwave irradiation: 15 min at 110 °C. After workup, the residue was purified by silica gel flash chromatography (EtOAc then EtOAc/MeOH 9:1). R_f = 0.64 (EtOAc/MeOH 9:1); $[\alpha]_D$ = −4.0 (c = 0.60 in CH_2Cl_2); ^{1}H NMR (400 MHz, $CDCl_3$): δ = 8.10–6.80 (m; H-ar, H-triaz), 5.37 (d, J = 2.5 Hz, 6H; H-4), 5.22–5.13 (m, 6H; H-2), 5.01 (dd, J = 10.5, 3.4 Hz, 6H; H-3), 4.62–4.45 (m, 18H; H-1, OCH_2CH_2N), 4.19–4.07 (m, 12H; H-6a, H-6b), 3.98–3.87 (m, 16H; H-5, 1×CH_2-EG$_3$), 3.86–3.76 (m, 6H; 1/2 GalOCH_2CH_2O), 3.73–3.64 (m, 6H; 1/2 GalOCH_2CH_2O), 3.55 (br s, 36H; 3×CH_2-EG$_3$), 2.13, 2.04, 2.03, 1.97 (4 s, 4×18H; CH_3CO), 1.30–0.80 ppm (m; 6×CMe_3); ^{13}C NMR (100 MHz, $CDCl_3$): δ = 170.5, 170.4, 170.3, 169.6 (4 s; 4×6C, 4×CH_3CO), 101.5 (C-1), 71.1 (C-3), 70.7 (C-5), 70.68, 70.62, 70.3 (3 s; 3×6C, 3×CH_2-EG$_3$), 69.6, 69.2 (2 s; 2×6C, GalOCH_2CH_2O, 1×CH_2-EG$_3$), 68.9 (C-2), 67.2 (C-4), 61.3 (C-6), 50.2 (OCH_2CH_2N), 31.6 ppm (br s, 18C; 6×CMe_3); HR-ESI-QTOF MS (positive mode): *m/z*: calcd for $C_{204}H_{282}N_{18}Na_2O_{78}$: 2138.9219 $[M+Na]^{2+}$; found: 2138.9302.

5,11,17,23,29,35-Hexa-*tert*-butyl-37,38,39,40,41,42-hexa({1-[(β-D-galactopyranosyloxy)-3,6-dioxaoct-8-yl]-1,2,3-triazol-4-yl}-4-methyleneoxy)calix[6]arene (15): Obtained as a freeze-dried pale-yellow solid (129 mg, 79%) by following method B: Compound **14** (215 mg, 51 μmol) was suspended in methanol (15 mL), water (3 mL) and triethylamine (3 mL). After stirring at RT for 4 days and concentration, the mixture was dissolved in ultra-pure water (5 mL) and then freeze-dried to afford the pure deacetylated glycocluster. $[\alpha]_D$ = +14.6 (c = 0.35 in H_2O); ^{1}H NMR (400 MHz, DMSO + εD_2O): δ = 8.40–7.10 (m; H-ar, H-triaz), 5.00–4.70 (m, 12H; OCH_2C-triaz), 4.60–4.40 (m, 12H; OCH_2CH_2N-triaz), 4.07 (m, 6H; H-1), 3.90–3.70 (m, 18H; OCH_2CH_2N, 1/2 GalOCH_2CH_2O), 3.60–3.40 (m, 70H; H-4, H-6a, H-6b, 1/2 GalOCH_2CH_2O, 3×CH_2-EG$_3$), 3.30–3.20 (m, 18H; H-2, H-3, H-5), 2.60–2.40 (m; Ar-CH_2-Ar), 1.20–0.60 ppm (m; 6×CMe_3); ^{13}C NMR (100 MHz, DMSO + εD_2O): δ = 103.7 (C-1), 75.3, 73.5, 70.6 (C-2, C-3, C-5), 70.0, 69.9, 69.8 (3 s; 3×6C, 3×CH_2-EG$_3$), 69.1 (OCH_2CH_2N), 68.2 (C-4), 68.0 (GalOCH_2CH_2O), 60.6 (C-6), 49.6 (OCH_2CH_2N), 46.0 (Ar-CH_2-Ar), 31.6 (br s; 18C, 6×C(CH_3)$_3$); HR-MALDI-TOF MS (positive-ion reflectron mode): *m/z*: calcd for $C_{156}H_{235}N_{18}O_{54}$: 3224.6191 $[M+H]^+$; found: 3224.6185.

5,10,15,20-Tetra(4-propargyloxy-phenyl) porphyrin (17):[66,67] Propionic acid (100 mL) was added to a 500 mL round-bottomed flask flushed with argon. The mixture was heated at 120 °C upon vigorous stirring and a mixture of *para*-propargyl-benzaldehyde (**16**)[68] (3.6 g, 22.5 mmol, 1 equiv) and pyrrole (1.6 mL, 22.5 mL, 1 equiv in 5 mL of propionic acid) was added dropwise. After 1 h, the mixture was cooled to RT (2 h). The crude product was precipitated by cooling the mixture with an ice-bath and adding methanol (250 mL). Filtration afforded a purple gum that was dissolved in dichloromethane. After evaporation and re-dissolution in a minimal quantity of chloroform, dropwise incorporation of methanol yielded the pure porphyrin **17** (1.09 g, 23%) as a deep-purple shiny solid. R_f = 0.49 (PE/CH_2Cl_2 1:1); ^{1}H NMR (300 MHz, $CDCl_3$): δ = 8.87 (s, 8H; H-porph), 8.14 (d, J = 8.4 Hz, 8H; H-ar), 7.36 (d, J = 8.4 Hz, 8H; H-ar), 4.98 (d, J = 1.9 Hz, 8H; OCH_2C≡CH), 2.70 (t, J = 1.9 Hz, 4H; C≡CH), −2.76 ppm (s, 2H; NH).

5,10,15,20-Tetra(4-propargyloxy-phenyl) porphyrin·Zn (18):[66,67] Porphyrin (**17**) (500 mg, 0.60 mmol, 1 equiv) and $ZnCl_2$ (410 mg, 3 mmol, 5 equiv) were introduced into a Biotage Initiator 2–5 mL vial. The vial was flushed with argon and protected from light (aluminium sheet). Anhydrous and degassed DMF (4.5 mL) and then Et_3N (585 μL, 4.2 mmol, 7 equiv) were added. The vial was sealed with a septum cap and heated at 120 °C for 15 min under microwave irradiation (solvent absorption

 © 2011 Wiley-VCH Verlag GmbH & Co. KGaA, Weinheim

level: high). After uncapping the vial, the crude mixture was diluted with EtOAc (250 mL). The organic layer was washed with water (3×100 mL) and brine (100 mL). The organic layer was dried (Na_2SO_4), filtered and evaporated. The crude product was crystallized ($CHCl_3$/MeOH) to afford the pure zinc–porphyrin **18** as shiny purple crystals (434 mg, 87%). R_f= 0.20 (PE/CH_2Cl_2 1:1); ^{1}H NMR (300 MHz, $CDCl_3$): δ=8.97 (s, 8H; H-porph), 8.14 (d, J=8.4 Hz, 8H; H-ar), 7.34 (d, J=8.4 Hz, 8H; H-ar), 4.97 (d, J=1.9 Hz, 8H; OCH_2C≡CH), 2.69 ppm (t, J=1.9 Hz, 4H, C≡CH).

5,10,15,20-Tetra{1-[(2,3,4,6-tetra-*O*-acetyl-β-D-galactopyranosyloxy)-3,6-dioxaoct-8-yl]-1,2,3-triazol-4-yl}-4-methyleneoxy-phenyl porphyrin·Zn (19): Obtained as a purple gum (104 mg, 64%) by following method A: Compound **18** (50 mg, 56 μmol, 1 equiv), **A** (169 mg, 0.34 mmol, 6 equiv), CuI (5.3 mg, 28 μmol, 0.5 equiv) and *i*Pr_2NEt (49 μL, 0.28 mmol, 5 equiv) in DMF (2.5 mL). After workup (without the washing with acidic solution), the residue was purified by silica gel flash chromatography (EtOAc then EtOAc/MeOH 95:5). R_f=0.30 (EtOAc/MeOH 9:1); ^{1}H NMR (300 MHz, $CDCl_3$): δ=8.92 (s, 8H; H-porph), 8.11 (d, J=8.5 Hz, 8H; H-ar), 7.72 (s, 4H; H-triaz), 7.25* (d, J=8.5 Hz, 8H; H-ar; signal partially overlapped by residual $CHCl_3$ peak), 5.34 (dd, J=3.3, <1 Hz, 4H; H-4), 5.18 (dd, J=10.5, 7.9 Hz, 4H; H-2), 4.97 (dd, J=10.5, 3.3 Hz, 4H; H-3), 4.86 (brs, 8H; PhOCH_2C-triaz), 4.50 (d, J=7.9 Hz, 4H; H-1), 4.41 (t, J= 4.9 Hz, 8H; OCH$_2$CH_2N-triaz), 4.15–4.02 (m, 8H; H-6a, H-6b), 3.98–3.89 (m, 4H; 1/2 GalOCH_2CH$_2$O), 3.88–3.83 (m, 4H; H-5), 3.79 (t, J=4.9 Hz, 8H; OCH_2CH$_2$N-triaz), 3.71–3.65 (m, 4H; 1/2 GalOCH_2CH$_2$O), 3.64–3.51 (m, 24H; GalOCH$_2$CH_2OCH_2CH_2O), 2.10, 2.00, 1.95, 1.94 ppm (4 s, 4× 12H; CH_3CO); ^{13}C NMR (75 MHz, $CDCl_3$): δ=170.5, 170.3, 170.2, 169.6 (4 s; CH_3CO), 157.9 (C^{IV}-ar), 150.5 (C^{IV}-porph), 143.7 (C^{IV}-triaz), 136.4 (C^{IV}-ar), 135.8 (CH-ar), 131.8 (CH-porph), 123.8 (CH-triaz), 120.4 (Ph-C^{IV}-porph), 112.9 (CH-ar), 101.4 (C-1), 71.0 (C-3), 70.8 (C-5), 70.8, 70.74, 70.68 (3 s; 12C; GalOCH$_2$CH_2OCH_2CH_2O), 69.4 (OCH_2CH$_2$N-triaz), 69.3 (GalOCH_2-), 68.9 (C-2), 67.1 (C-4), 62.0 (PhOCH_2C-triaz), 61.3 (C-6), 50.4 (OCH$_2$CH_2N-triaz), 20.9, 20.8, 20.74, 20.70 (4 s; CH_3CO); MALDI-TOF MS (positive-ion reflectron mode): m/z: calcd for $C_{136}H_{160}N_{16}O_{52}Zn$: 2912.97 $[M]^+$; found 2912.92.

5,10,15,20-Tetra{1-[(β-D-galactopyranosyloxy)-3,6-dioxaoct-8-yl]-1,2,3-triazol-4-yl}-4-methyleneoxy-phenyl porphyrin·Zn (20): Obtained as a freeze-dried purple foam (66 mg, 99%) by following method B: Compound **19** (86 mg, 29 Mmol) was suspended in methanol (5 mL), dichloromethane (1 mL), water (1 mL) and triethylamine (1 mL). After stirring at RT for 4 days and concentration, the mixture was dissolved in ultrapure water (5 mL) and then freeze-dried to afford the pure deacetylated glycocluster. ^{1}H NMR (400 MHz, DMSO+εD$_2$O): δ=8.81 (s, 8H; H-porph), 8.39 (s, 4H; H-triaz), 8.09 (d, J=8.5 Hz, 8H; H-ar), 7.47 (d, J= 8.5 Hz, 8H; H-ar), 5.44 (brs, 8H; PhOCH_2C-triaz), 4.64 (t, J=5.1 Hz, 8H; OCH$_2$CH_2N-triaz), 4.12 (d, J=7.2 Hz, 4H; H-1), 3.92 (t, J=5.1 Hz, 8H; OCH_2CH$_2$N-triaz), 3.89–3.80 (m, 4H; H-6a), 3.64–3.46 (m, 40H; H-5, H-6b, GalOCH_2CH_2OCH_2CH_2O), 3.38–3.23 ppm (m, 12H; H-2, H-3, H-4); ^{13}C NMR (100 MHz, DMSO+εD$_2$O): δ=157.8 (C^{IV}-ar), 149.7 (C^{IV}-porph), 142.8 (C^{IV}-triaz), 135.4 (C^{IV}-ar), 135.3 (CH-ar), 131.7 (CH-porph), 125.4 (CH-triaz), 120.0 (Ph-C^{IV}-porph), 113.0 (CH-ar), 103.66 (C-1), 75.2, 73.4, 70.5 (3 s, C-2, C-3, C-4), 69.9, 69.8, 69.7 (3 s, 12C; GalOCH$_2$CH$_2$OCH_2CH_2O), 68.9 (OCH_2CH$_2$N-triaz), 68.1 (C-5), 67.9 (C-6), 61.5 (PhOCH_2C-triaz), 60.5 (GalOCH_2-), 49.7 ppm (OCH$_2$CH_2N-triaz); MALDI-TOF MS (positive-ion reflectron mode): calcd for $C_{104}H_{128}N_{16}O_{36}Zn$: 2240.80 $[M]^+$; found: 2240.78.

Hemagglutination inhibition assays (HIA): Hemagglutination inhibition assays were performed in U-shaped 96-well microtitre plates. Rabbit erythrocytes were bought from Biomerieux and used without further washing. The erythrocytes were diluted to a 4% solution in NaCl (150 mM). Lectin solutions of 2 mg/mL were prepared in Tris/HCl (20 mM), NaCl (100 mM) and $CaCl_2$ (100 μM). The hemagglutination unit (HU) was first obtained by the addition of 25 μL of the 4% erythrocyte solution to 25 μL aliquots of sequential (two-fold) lectin dilutions. The mixture was incubated at 25°C for 60 min. The HU was measured as the minimum lectin concentration required to prevent hemagglutination. For the following lectin-inhibition assays, lectin concentrations of four times that of the hemagglutination unit were used. For PA-IL, this concentration was found to be 6 and 20 μg/mL for ECA. Subsequent assays were then carried out by the addition of 12.5 μL lectin solution (at the required concentration) to 25 μL of sequential dilutions of glycoclusters, monomer molecules and controls. These solutions were then incubated at 25°C for 2 h and then 12.5 μL of 4% erythrocyte solution was added followed by an additional incubation at 25°C for 30 min. The minimum inhibitory concentration for each molecule was determined by simple eye detection.

Surface plasmon resonance studies (SPR): SPR inhibition experiments were performed on a Biacore 3000 instrument at 25°C. Measurements were carried out on 2 channels with 2 immobilised sugars: α-L-fucose (channel 1), α-D-galactose (channel 2). Immobilization of sugars was performed at 25°C by using running buffer (HBS) at 5 μL min^{-1}. Immobilization on each channel (CM5 Chip) was performed independently as follows. First, channel was activated by injecting a fresh mixture of EDC/NHS (35 μL, 420 s). Then, a solution of strepatavidin (100 μg/mL in Na acetate pH 5 buffer) was injected (50 μL, 600 s). Remaining reactive species were quenched by injecting ethanolamine (1 M, 35 μL, 420 s). Finally a solution of the desired biotinylated–polyacrylamide–sugar (Lectinity, 200 μg/mL) was coated onto the surface (50 μL, 600 s) through streptavidin–biotin interaction. This procedure led to 804 RU (fucoside) and 796 RU (galactoside) of immobilized sugars on channel 1 and 2, respectively. Inhibition experiments were performed with the galactosylated channel 2 and plots represent substracted data (channel 2–channel 1).

Conditions for ECA: The running buffer for ECA experiments is HEPES (10 mM), $CaCl_2$ (2 mM), $MnCl_2$ (2 mM), Tween P20 0.005%, pH 7.4. Inhibition studies consisted in the injection (50 μL, 10 μL min^{-1}, dissociation: 60 s) of incubated (>1 h, RT) mixtures of ECA (0.5 μM) and various concentrations of inhibitor (2-fold cascade dilutions). For each inhibition assay, ECA (0.5 μM) without inhibitor was injected to observe the full adhesion of the lectin onto the sugar-coated surface (0% inhibition). The CM5 chip was fully regenerated by successive injections of D-galactose (10 μL, 100 mM in running buffer) and NaCl (2×10 μL, 1 M in running buffer).

Conditions for PA-IL: The running buffer for PA-IL experiments is HEPES (10 mM), NaCl (150 mM), $CaCl_2$ (10 mM), Tween P20 0.005%, pH 7.4. Inhibition studies consisted in the injection (150 μL, 10 μL min^{-1}, dissociation: 120 s) of incubated (>1 h, RT) mixtures of PA-IL (5 μM) and various concentrations of inhibitor (2-fold cascade dilutions). For each inhibition assay, PA-IL (5 μM) without inhibitor was injected to observe the full adhesion of the lectin onto the sugar-coated surface (0% inhibition). The CM5 chip was fully regenerated by successive injections of D-galactose (2×30 μL, 100 mM in running buffer).

For both experimental settings, binding was measured as RU over time after blank subtraction, and data were then evaluated by using the BIAevaluation Software, Version 4.1. For IC_{50} evaluation, the response (Req-fitted) was considered as the amount of lectin bound to the sugar surface at equilibrium in the presence of a defined concentration of inhibitor. Inhibition curves were obtained by plotting the percentage of inhibition against the inhibitor concentration (on a logarithmic scale) by using Origin 7.0 software (OriginLab Corp.) and IC_{50} values were extracted from a sigmoidal fit of the inhibition curve.

Isothermal titration microcalorimetry (ITC): Recombinant lyophilized PA-IL was dissolved in buffer (0.1 M Tris-HCl, 6 μM $CaCl_2$, pH 7.5) and degassed (see the Supporting Information for concentration details). Protein concentration was checked by measurement of optical density by using a theoretical molar extinction coefficient of 28000. Carbohydrate ligands were dissolved directly into the same buffer, degassed, and placed in the injection syringe. ITC was performed with a VP-ITC MicroCalorimeter from MicroCal Incorporated. PA-IL was placed into the 1.4478 mL sample cell, at 25°C. Titration was performed with 10 μL injections of carbohydrate ligands every 300 s. Data were fitted with MicroCal Origin 7 software, according to standard procedures. Fitted data yielded the stoichiometry (n), the association constant (K_a) and the enthalpy of binding (ΔH). Other thermodynamic parameters (i.e. changes in free energy, ΔG, and entropy, ΔS) were calculated from the equation $\Delta G=\Delta H-T\Delta S=-RT\ln K_a$ in which T is the absolute temperature and R=8.314 J mol^{-1} K^{-1}. Two or three independent titrations were performed for each ligand tested.

 © 2011 Wiley-VCH Verlag GmbH & Co. KGaA, Weinheim

Acknowledgements

The authors thank the Université Claude Bernard Lyon 1, Université Blaise Pascal-Clermont-Ferrand II and the CNRS for financial support. S.C. thanks the Région Rhône-Alpes (Cluster de Recherche Chimie) and the CNRS (Programme Interdisciplinaire: Chimie pour le Développement Durable) for additional funding. Financial help is acknowledged from Vaincre la Mucovisdicose and GDR Pseudomonas. A.I. acknowledges funding from ANR Glycoasterix. M.W. acknowledges the Czech Ministry of Education (MSM0021622413, ME08008). Part of the research has received funding from the European Community's Seventh Framework Programme under grant agreement no. 205872. Dr D. Bouchu, C. Duchamp and N. Henriques are gratefully acknowledged for mass spectrometry analyses.

[1] H. Lis, N. Sharon, *Chem. Rev.* **1998**, *98*, 637–674.
[2] R. T. Lee, Y. Ichikawa, T. Kawasaki, K. Drickamer, Y. C. Lee, *Arch. Biochem. Biophys.* **1992**, *299*, 129–136.
[3] Y. C. Lee, R. T. Lee, *Acc. Chem. Res.* **1995**, *28*, 321–327.
[4] J. J. Lundquist, E. J. Toone, *Chem. Rev.* **2002**, *102*, 555–578.
[5] Y. M. Chabre, R. Roy, *Adv. Carbohydr. Chem. Biochem.* **2010**, *63*, 165–393.
[6] C. Carpenter, S. A. Nepogodiev, *Eur. J. Org. Chem.* **2005**, 3286–3296.
[7] S. Dedola, S. A. Nepogodiev, R. A. Field, *Org. Biomol. Chem.* **2007**, *5*, 1006–1017.
[8] M. Dubber, O. Sperling, T. K. Lindhorst, *Org. Biomol. Chem.* **2006**, *4*, 3901–3912.
[9] D. A. Fulton, J. F. Stoddart, *J. Org. Chem.* **2001**, *66*, 8309–8319.
[10] A. Nelson, J. M. Belitsky, S. Vidal, C. S. Joiner, L. G. Baum, J. F. Stoddart, *J. Am. Chem. Soc.* **2004**, *126*, 11914–11922.
[11] V. Wittmann, S. Seeberger, *Angew. Chem.* **2004**, *116*, 918–921; *Angew. Chem. Int. Ed.* **2004**, *43*, 900–903.
[12] M. J. Cloninger, *Curr. Opin. Chem. Biol.* **2002**, *6*, 742–748.
[13] S. A. Nepogodiev, J. F. Stoddart, *Adv. Macromol. Carbohydr. Res.* **2003**, *2*, 191–239.
[14] R. Roy, *Trends Glycosci. Glycotechnol.* **2003**, *15*, 291–310.
[15] S. L. Flitsch, *Current Opinion in Chemical Biology* **2000**, *4*, 619–625.
[16] S.-I. Nishimura, Y. C. Lee in *Polysaccharides: Structural Diversity and Functional Versatility* (Ed.: S. Dimitriu), Marcel Dekker, New York, **1998**, pp. 523–537.
[17] R. Roy in *Carbohydrate Chemistry* (Ed.: G.-J. Boons), Blackie, London, **1998**, pp. 243–321.
[18] J. M. de La Fuente, S. Penadés, *Biochim. Biophys. Acta Gen. Subj.* **2006**, *1760*, 636–651.
[19] A. Carvalho de Souza, J. F. G. Vliegenthart, J. P. Kamerling, *Org. Biomol. Chem.* **2008**, *6*, 2095–2102.
[20] R. Narain, A. Housni, G. Gody, P. Boullanger, M.-T. Charreyre, T. Delair, *Langmuir* **2007**, *23*, 12835–12841.
[21] C. L. Schofield, A. H. Haines, R. A. Field, D. A. Russell, *Langmuir* **2006**, *22*, 6707–6711.
[22] M. Marradi, M. Martín-Lomas, S. Penadés, H. Derek, *Adv. Carbohydr. Chem. Biochem.* **2010**, *64*, 211–290.
[23] S. André, F. Sansone, H. Kaltner, A. Casnati, J. Kopitz, H. J. Gabius, R. Ungaro, *ChemBioChem* **2008**, *9*, 1649–1661.
[24] S. Cecioni, R. Lalor, B. Blanchard, J.-P. Praly, A. Imberty, S. E. Matthews, S. Vidal, *Chem. Eur. J.* **2009**, *15*, 13232–13240.
[25] T. K. Dam, S. Oscarson, R. Roy, S. K. Das, D. Pagé, F. Macaluso, C. F. Brewer, *J. Biol. Chem.* **2004**, *280*, 8640–8646.
[26] J. E. Gestwicki, C. W. Cairo, L. E. Strong, K. A. Oetjen, L. L. Kiessling, *J. Am. Chem. Soc.* **2002**, *124*, 14922–14933.
[27] M. Lahmann, *Top. Curr. Chem.* **2009**, *288*, 17–65.
[28] B. Blanchard, A. Nurisso, E. Hollville, C. Tétaud, J. Wiels, M. Pokorná, M. Wimmerová, A. Varrot, A. Imberty, *J. Mol. Biol.* **2008**, *383*, 837–853.
[29] A. Nurisso, B. Blanchard, A. Audfray, L. Rydner, S. Oscarson, A. Varrot, A. Imberty, *J. Biol. Chem.* **2010**, *285*, 20316–20327.
[30] G. Cioci, E. P. Mitchell, C. Gautier, M. Wimmerova, D. Sudakevitz, S. Perez, N. Gilboa-Garber, A. Imberty, *FEBS Lett.* **2003**, *555*, 297–301.
[31] C. Svensson, S. Teneberg, C. L. Nilsson, A. Kjellberg, F. P. Schwarz, N. Sharon, U. Krengel, *J. Mol. Biol.* **2002**, *321*, 69–83.
[32] H. C. Kolb, M. G. Finn, K. B. Sharpless, *Angew. Chem.* **2001**, *113*, 2056–2075; *Angew. Chem. Int. Ed.* **2001**, *40*, 2004–2021.
[33] V. V. Rostovtsev, L. G. Green, V. V. Fokin, K. B. Sharpless, *Angew. Chem.* **2002**, *114*, 2708–2711; *Angew. Chem. Int. Ed.* **2002**, *41*, 2596–2599.
[34] Q. Wang, T. R. Chan, R. Hilgraf, V. V. Fokin, K. B. Sharpless, M. G. Finn, *J. Am. Chem. Soc.* **2003**, *125*, 3192–3193.
[35] P. Wu, M. Malkoch, J. N. Hunt, R. Vestberg, E. Kaltgrad, M. G. Finn, V. V. Fokin, K. B. Sharpless, C. J. Hawker, *Chem. Commun.* **2005**, 5775–5777.
[36] M. Meldal, C. W. Tornoe, *Chem. Rev.* **2008**, *108*, 2952–3015.
[37] C. W. Tornoe, C. Christensen, M. Meldal, *J. Org. Chem.* **2002**, *67*, 3057–3064.
[38] C. Bouillon, A. Meyer, S. Vidal, A. Jochum, Y. Chevolot, J. P. Cloarec, J. P. Praly, J. J. Vasseur, F. Morvan, *J. Org. Chem.* **2006**, *71*, 4700–4702.
[39] F. Morvan, A. Meyer, A. Jochum, C. Sabin, Y. Chevolot, A. Imberty, J.-P. Praly, J.-J. Vasseur, E. Souteyrand, S. Vidal, *Bioconjugate Chem.* **2007**, *18*, 1637–1643.
[40] Y. Chevolot, C. Bouillon, S. Vidal, F. Morvan, A. Meyer, J.-P. Cloarec, A. Jochum, J.-P. Praly, J.-J. Vasseur, E. Souteyrand, *Angew. Chem.* **2007**, *119*, 2450–2454; *Angew. Chem. Int. Ed.* **2007**, *46*, 2398–2402.
[41] F. Fazio, M. C. Bryan, O. Blixt, J. C. Paulson, C. H. Wong, *J. Am. Chem. Soc.* **2002**, *124*, 14397–14402.
[42] F. Pérez-Balderas, M. Ortega-Munoz, J. Morales-Sanfrutos, F. Hernandez-Mateo, F. G. Calvo-Flores, J. A. Calvo-Asin, J. Isac-Garcia, F. Santoyo-Gonzalez, *Org. Lett.* **2003**, *5*, 1951–1954.
[43] B. C. Hamper, S. A. Kolodziej, A. M. Scates, R. G. Smith, E. Cortez, *J. Org. Chem.* **1998**, *63*, 708–718.
[44] O. Roy, S. Faure, V. Thery, C. Didierjean, C. Taillefumier, *Org. Lett.* **2008**, *10*, 921–924.
[45] J. M. Holub, K. Kirshenbaum, *Chem. Soc. Rev.* **2010**, *39*, 1325–1337.
[46] C. Schilling, N. Jung, S. Bräse in *Click Chemistry for Biotechnology and Materials Science* (Ed.: J. Lahann), Wiley, Chichester, **2009**, pp. 9–28.
[47] A. Dondoni, *Chem. Asian J.* **2007**, *2*, 700–708.
[48] Z. Szurmai, L. Szabó, A. Lipták, *Acta Chim. Hung.* **1989**, *126*, 259–269.
[49] R. Roy, J. M. Kim, *Angew. Chem.* **1999**, *111*, 380–384; *Angew. Chem. Int. Ed.* **1999**, *38*, 369–372.
[50] A. Marra, M.-C. Scherrmann, A. Dondoni, R. Ungaro, A. Casnati, P. Minari, *Angew. Chem., Int. Ed. Engl.* **1995**, *33*, 2479–2481.
[51] A. Dondoni, A. Marra, M.-C. Scherrmann, A. Casnati, F. Sansone, R. Ungaro, *Chem. Eur. J.* **1997**, *3*, 1774–1782.
[52] A. Dondoni, M. Kleban, X. Hu, A. Marra, H. D. Banks, *J. Org. Chem.* **2002**, *67*, 4722–4733.
[53] S. P. Bew, R. A. Brimage, N. L'Hermite, S. V. Sharma, *Org. Lett.* **2007**, *9*, 3713–3716.
[54] A. Dondoni, M. Kleban, A. Marra, *Tetrahedron Lett.* **1997**, *38*, 7801–7804.
[55] C. Félix, H. Parrot-Lopez, V. Kalchenko, A. W. Coleman, *Tetrahedron Lett.* **1998**, *39*, 9171–9174.
[56] Z. Asfari, V. Bohmer, J. Harrowfield, J. Vicens, *Calixarenes 2001*, Kluwer Academic Publishers, Dordrecht, **2001**.
[57] R. G. Janssen, W. Verboom, D. N. Reinhoudt, A. Casnati, M. Freriks, A. Pochini, F. Ugozzoli, R. Ungaro, P. M. Nieto, M. Carramolino, F. L. Cuevas, P. Prados, J. de Mendoza, *Synthesis* **1993**, 380–386.
[58] J. P. M. van Duynhoven, R. G. Janssen, W. Verboom, S. M. Franken, A. Casnati, A. Pochini, R. Ungaro, J. de Mendoza, P. M. Nieto, *J. Am. Chem. Soc.* **1994**, *116*, 5814–5822.
[59] S. Kanamathareddy, C. D. Gutsche, *J. Org. Chem.* **1994**, *59*, 3871–3879.

 © 2011 Wiley-VCH Verlag GmbH & Co. KGaA, Weinheim

[60] C. Kaldapa, J. C. Blais, V. Carré, R. Granet, V. Sol, M. Guilloton, M. Spiro, P. Krausz, *Tetrahedron Lett.* **2000**, *41*, 331–335.
[61] V. Sol, J. C. Blais, G. Bolbach, V. Carré, R. Granet, M. Guilloton, M. Spiro, P. Krausz, *Tetrahedron Lett.* **1997**, *38*, 6391–6394.
[62] V. Sol, J. C. Blais, V. Carre, R. Granet, M. Guilloton, M. Spiro, P. Krausz, *J. Org. Chem.* **1999**, *64*, 4431–4444.
[63] V. Sol, P. Branland, R. Granet, C. Kaldapa, B. Verneuil, P. Krausz, *Bioorg. Med. Chem. Lett.* **1998**, *8*, 3007–3010.
[64] V. Sol, V. Chaleix, Y. Champavier, R. Granet, Y. M. Huang, P. Krausz, *Bioorg. Med. Chem.* **2006**, *14*, 7745–7760.
[65] V. Sol, V. Chaleix, R. Granet, P. Krausz, *Tetrahedron* **2008**, *64*, 364–371.
[66] Y. Liu, C.-F. Ke, H.-Y. Zhang, J. Cui, F. Ding, *J. Am. Chem. Soc.* **2008**, *130*, 600–605.
[67] M. A. Olson, A. Coskun, R. Klajn, L. Fang, S. K. Dey, K. P. Browne, B. A. Grzybowski, J. F. Stoddart, *Nano Lett.* **2009**, *9*, 3185–3190.
[68] M. Pal, K. Parasuraman, K. R. Yeleswarapu, *Org. Lett.* **2003**, *5*, 349–352.
[69] J.-S. Marois, K. Cantin, A. Desmarais, J.-F. Morin, *Org. Lett.* **2008**, *10*, 33–36.
[70] G. Costa, E. Reisenhofer, L. Stefani, *J. Inorg. Nucl. Chem.* **1965**, *27*, 2581–2584.
[71] C. Chemani, A. Imberty, S. de Bentzmann, M. Pierre, M. Wimmerova, B. P. Guery, K. Faure, *Infect. Immun.* **2009**, *77*, 2065–2075.
[72] B. Blanchard, PhD Thesis, Etudes structurales et fonctionnelles de Lectines et adhésines chez Pseudomonas aeruginosa, CERMAV, Université Joseph Fourier Grenoble **2009**.
[73] T. K. Dam, T. A. Gerken, C. F. Brewer, *Biochemistry* **2009**, *48*, 3822–3827.
[74] J. B. Corbell, J. J. Lundquist, E. J. Toone, *Tetrahedron: Asymmetry* **2000**, *11*, 95–111.

Received: September 13, 2010
Published online: January 5, 2011

 © 2011 Wiley-VCH Verlag GmbH & Co. KGaA, Weinheim